Structure and function of the pore canals of the sea urchin madreporite

MASAKI TAMORI[1], AKIRA MATSUNO[2] AND KEIICHI TAKAHASHI[3]*

[1] *Biological Laboratory, Faculty of Science, Tokyo Institute of Technology, O-okayama, Tokyo 152, Japan*
[2] *Department of Biology, Shimane University, Nishikawazu, Matsue 690, Japan*
[3] *Department of Biology, International Christian University, Mitaka, Tokyo 181, Japan*

SUMMARY

The madreporite is one of the most enigmatic organs of the echinoderms. It connects the internal cavity of the water-vascular system to the external seawater through its many pores which are lined with ciliated epithelium. Its physiological function, even the nature of transport, if any, through its pores has been controversial since the 19th century. We report here that the pores of the echinoid madreporite are capable of changing their diameter in response to stimulation and that their cilia support bidirectional transport, drawing water into the water-vascular system while expelling larger particles. A reversible constriction of the pore was induced by acetylcholine (ACh). At $> 10^{-7}$ M, ACh reduced the pore diameter to about 70% in 2 mins and to 60% in 6 mins. Atropine (10^{-4} M), but not *d*-tubocurarine (10^{-4} M), blocked the response to ACh (10^{-7} M). Adrenaline (10^{-5} M) had no effect on the pore diameter. These results suggest that the size of the pore is under cholinergic control. Observations of isolated pore-canal tissue indicated that the changes in pore size are not accompanied by changes in volume of the cells surrounding the pores. Electron microscopy showed no muscle cells in or near the pore-canal tissue. In the apical region of the ciliated columnar epithelial cell lining the pore canal, there are fine filaments attached to the adherens junctions. This region of the cell was positively stained with rhodamine-phalloidin, suggesting that the filaments consist of F-actin. It is possible that the filaments are involved in the pore closure response. We studied the water flow through isolated single pore canals, using Indian ink, and found that the water flows inwards while particles larger than ca. 1 μM move in the opposite direction. When the pores became narrower by the action of ACh, complete blocking of the water flow was observed. It is possible that the madreporite controls the volume or the pressure of the fluid in the water-vascular system by both the ciliary-driven water flow and the pore closure response.

1. INTRODUCTION

The water-vascular system is a distinctive feature of echinoderms. Owing largely to the activity of its numerous tube feet, it serves such vital functions as locomotion, feeding, respiration etc. In most cases, the internal cavity of the water-vascular system is open to the external seawater through the many ciliated pores of an organ called the madreporite situated at the aboral end of the stone canal. Because the tube feet are hydraulic organs, it would seem that the madreporite serves to regulate the pressure and/or the volume of the fluid in the water-vascular system. Despite the many observations and experiments carried out since the 19th century (Nichols 1966), however, the function of the madreporite has been controversial. This is largely due to the conflicting observations on the water flow through the madreporite.

Thus some investigators reported that water flows outwards through the madreporite or the larval pore canal based on their observations of the movement of particles suspended in seawater (Hartog 1887; Ruppert & Balser 1986). These investigators suggested that the madreporite functions as an excretory organ. However, other investigators, also using suspended particles to determine the direction of water flow, concluded that the water flows inwards (Ludwig 1890; MacBride 1896).

Gemmill (1914) and Budington (1942) reported that the cilia in the pore canal beat in an outward direction while those in the stone canal beat in the opposite direction. They both suggested that the current in the pore canal is directed inwards. Gemmill (1914) suggested that the current in the pore canal is not strong enough to compete with that in the stone canal so that water enters from the outside into the water-vascular system. He thought that the cilia in the pore canal prevent the entry of foreign particles. Some investigators studied whether the animals incorporate such substances as dyes, radioisotopes and fluorescent tracers into the water-vascular system to see if the inflow of seawater occurs through the madreporite (Bargmann & Behrens 1964; Binyon 1964; Prusch & Whoriskey 1976; Prusch 1977; Ferguson 1984, 1988, 1989, 1990). Their results are conflicting. Bargmann & Behrens (1964) and Ferguson (1984, 1988, 1989, 1990)

* Author to whom correspondence should be addressed.

reported that incorporation of the substances occurred whereas Binyon (1964), Prusch & Whoriskey (1976) and Prusch (1977) failed to show such incorporation. Ferguson (1984, 1988, 1989, 1990, 1992) suggested that the inflow of the external seawater is responsible for the regulation of the volume of the fluid in the main body cavity rather than that in the water-vascular system.

Fechter (1965), using a manometer, observed no water flow across the madreporite of *Echinus esculentus* in 24 h while the tube feet were showing their normal activity. He also found that the movement of the tube feet was inhibited when a pressure which was either higher or lower than that of the external seawater was applied on the madreporite. He suggested that the madreporite functions as a pressure equalizer between the outside and the inside of the water-vascular system.

For this study we carried out experiments and made detailed observations, with the aim of understanding the function of echinoid madreporites. We found that the pores of the madreporite constrict reversibly in response to stimulation. This finding indicates that the soft tissue surrounding the madreporic pores can regulate the transport of substances through the madreporite. Observations on the isolated soft tissue (pore tube), electron microscopy and rhodamine-phalloidin staining suggested that the pore closure response is caused by constriction of the apical region of the pore-canal cells. Using the isolated pore tubes, we found that water flows inwards through the pore canal while particles suspended in the water are transported in the opposite direction. These observations solved the controversies regarding the direction of water movement and provided clues to the function of the madreporite.

Preliminary results of this study have been published in abstract forms (Takahashi *et al.* 1987, 1991; Takahashi & Tamori 1988; Tamori *et al.* 1990, 1991*a*, *b*, *c*; Tamori & Takahashi 1992).

2. MATERIALS AND METHODS

(*a*) *Animals*

For most of the experiments we used the regular echinoid, *Hemicentrotus pulcherrimus*. Other regular echinoids, *Pseudocentrotus depressus*, *Anthocidaris crassispina* and *Temnopleurus toreumaticus* were used for the study with a scanning electron microscope (SEM). The urchins were collected near the Misaki Marine Biological Station and were either used immediately or were maintained in an aquarium for up to two months until use.

(*b*) *Scanning electron microscopy*

For observation with a SEM, a piece of test material which included the madreporite was cut from the sea urchin, washed in deionized water and immersed in a solution containing NaClO (a commercial bleach, 'Coop Bleach' diluted to 1/4 with deionized water) to remove the soft tissues ('cleaning'). It was then washed in deionized water, immersed in 70% ethanol, air-dried and coated with gold with a sputter coater (IB-3, Eiko Engineering) and observed with a SEM (JSM-T220, Japan Electronics Optics Laboratory). Observation was also made with a low-vacuum SEM (WS-250, 'WET-SEM', Topcon Ltd.) which enabled us to examine fresh, unfixed and uncoated madreporites without much damage (Shimakura & Robinson 1989).

(*c*) *Transmission electron microscopy*

For observation with a transmission electron microscope (TEM), a thin piece of the tissue (less than 0.5 mm in thickness) was sliced off the aboral surface of the madreporite and fixed according to Eakin & Brandenburger (1979) with some modifications. All the steps of fixation were carried out on ice. The tissue was initially treated for 1 min with 2% OsO_4 in artificial seawater (ASW) consisting of 430 mM NaCl, 10 mM KCl, 10 mM $CaCl_2$, 50 mM $MgCl_2$, and 10 mM Tris (tris(hydroxymethyl)-aminomethane) (pH 8.0). The tissue was then immersed in a solution containing 4% glutaraldehyde, 0.2 M sodium cacodylate, 0.1 M NaCl, and 0.35 M sucrose (pH 7.2) for 2 h. After this, it was rinsed for 1 h in a solution containing 0.2 M sodium cacodylate and 0.32 M NaCl, and postfixed in a solution containing 1% OsO_4, 0.1 M sodium cacodylate and 0.16 M NaCl for 2 h.

Some specimens were treated before fixation with 10^{-4}–10^{-5} M carbachol (CCh; Sigma Chemicals Co.), a synthetic analogue of acetylcholine (ACh), to induce the pore closure response.

The fixed specimens were rinsed three times (5 mins each) in 0.3 M NaCl and decalcified in a 1:1 mixture of 2% ascorbic acid and 0.3 M NaCl for 12–24 h (Dietrich & Fontaine 1975). They were then dehydrated with a graded series of ethanol and embedded in an epoxy resin (TAAB 812, TAAB Laboratories Equipment Ltd).

Ultra-thin sections were stained with 4% uranyl acetate followed by 0.4% lead citrate (Venable & Coggeshall 1965) and examined with a transmission electron microscope (100-CX, Japan Electronics Optics Laboratory).

(*d*) *Experiments using isolated madreporite*

To study the effects of chemicals on the external openings of the madreporite, a thin (less than 0.5 mm) piece of tissue was sliced off the aboral surface of the madreporite with a razor blade. The piece was then fixed to the bottom of a seawater-filled perfusion chamber (capacity 170 μl) with a small clamp made of a silicone plate and a stainless-steel wire. The chamber had acrylic walls and a bottom of a glass slide permitting observation with transmitted light. A Nikon microscope with a 20× water-immersion lens (W-20, Nikon; N.A. = 0.33) was used to observe the external openings of the madreporite. Photomicrographs were taken with a 35 mm camera and used for analysing the responses of the madreporite. The effects of the following chemicals were studied: acetylcholine chloride (ACh; Nakarai Chemicals), adrenaline (Adr; E. Merck), atropine sulfate (Wako Chemicals), *d*-tubocurarine chloride (*d*-TC; Nakarai Chemicals), and ASW containing a high concentration of K^+. The drugs were dissolved in ASW and injected into an end of

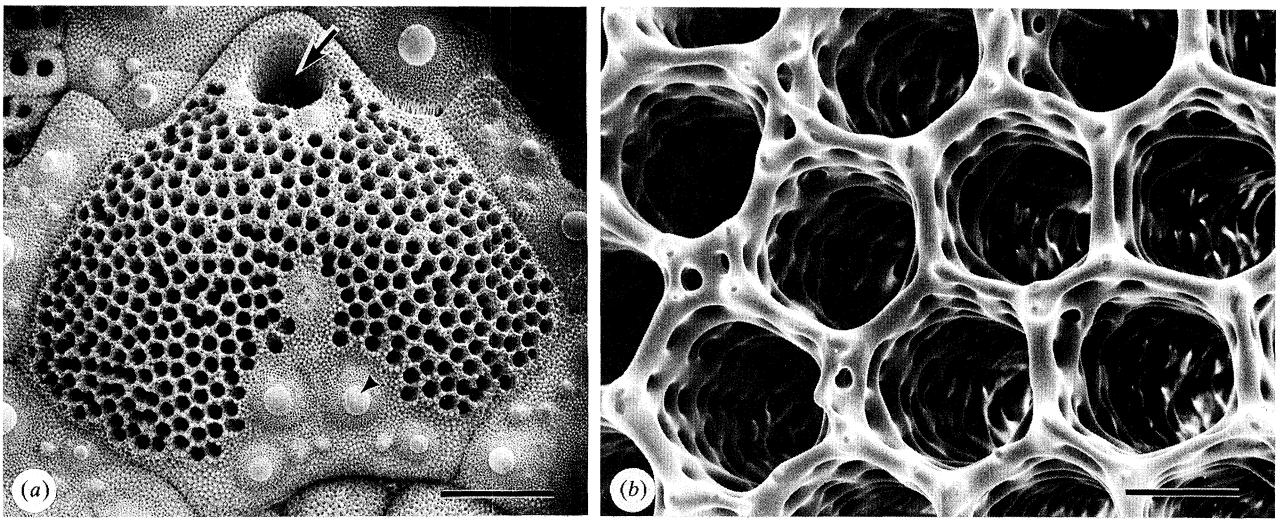

Figure 1. Outside (aboral) views of a madreporic ossicle of *Hemicentrotus pulcherrimus* (ambital diameter: 2.8 cm). (*a*) The whole ossicle: the arrow indicates the gonopore, the arrowhead indicates a spine base. Bar represents 500 μm. (*b*) A part of (*a*) at higher magnification. Bar represents 50 μm.

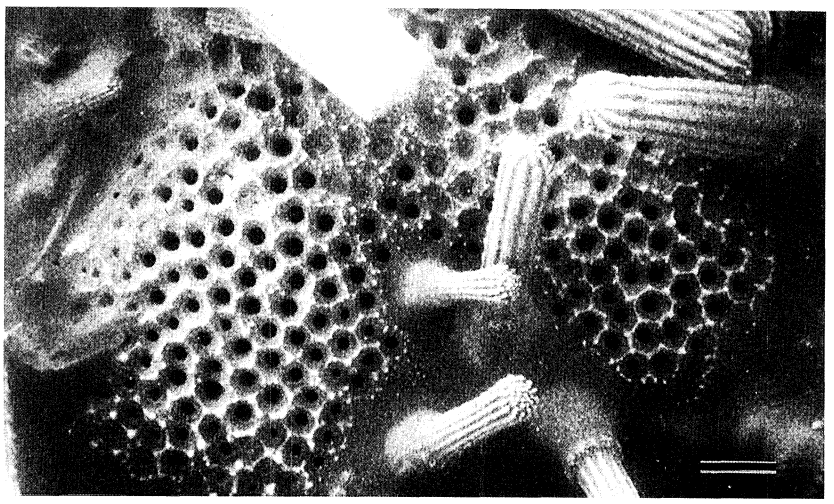

Figure 2. An outside (aboral) view of a fresh, unfixed and uncoated madreporite of *Hemicentrotus pulcherrimus* (ambital diameter: 2.2 cm) observed with a 'WET-SEM'. Bar represents 200 μm.

the chamber for 10 s at a constant rate (50 μl s^{-1}) through a silicone tube using a peristaltic pump, followed by a prolonged perfusion with ASW. During the experiment, excess solution was drained from the opposite end with a stainless-steel tube connected to a suction pump. The experiments were carried out at room temperature (21–27 °C).

(*e*) *Experiments using an isolated single pore canal*

To observe the soft tissue lining the madreporic pores ('pore tubes') in profile, we isolated a single pore tube. A thin piece of the tissue sliced off the external surface of the madreporite was treated with ASW containing 0.2% collagenase (135–264 units per mg; Type II, Worthington Biochemical Co.) for 1 h at 30 °C with constant shaking at a rate of 100 per min to dissolve the basal lamina between the soft tissue and the ossicle. Then the soft tissue, consisting of several pore tubes connected by the aboral epithelial tissue, was separated from the ossicle by gentle lifting with an eyelash. To isolate a single pore tube, the epithelium was cut with a glass needle between the tube. The isolated tubes were attached on a polylysine-coated glass slide between two strips of adhesive tape (Nichiban, 'Nice-Tak') used as spacers and observed with a differential interference contrast microscope (NTF, Nikon) under a cover slip. Test solutions were perfused by adding it from one side of the cover slip and blotting it from the opposite side with a piece of filter paper.

To study the water movement in the pore canal, we used colloidal carbon (Indian ink). The ink was dialysed overnight against distilled water. After the dialysis, the ink was centrifuged at 12000 *g* for 10 mins. The supernatant was used after it had been diluted with the same volume of the double strength ASW. Before the dilution, we measured the size of the carbon particles in the ink using a transmission electron microscope. Our observation showed that the carbon particles usually formed clumps. The diameter of the particle or the clump was usually 150–500 nm. Some-

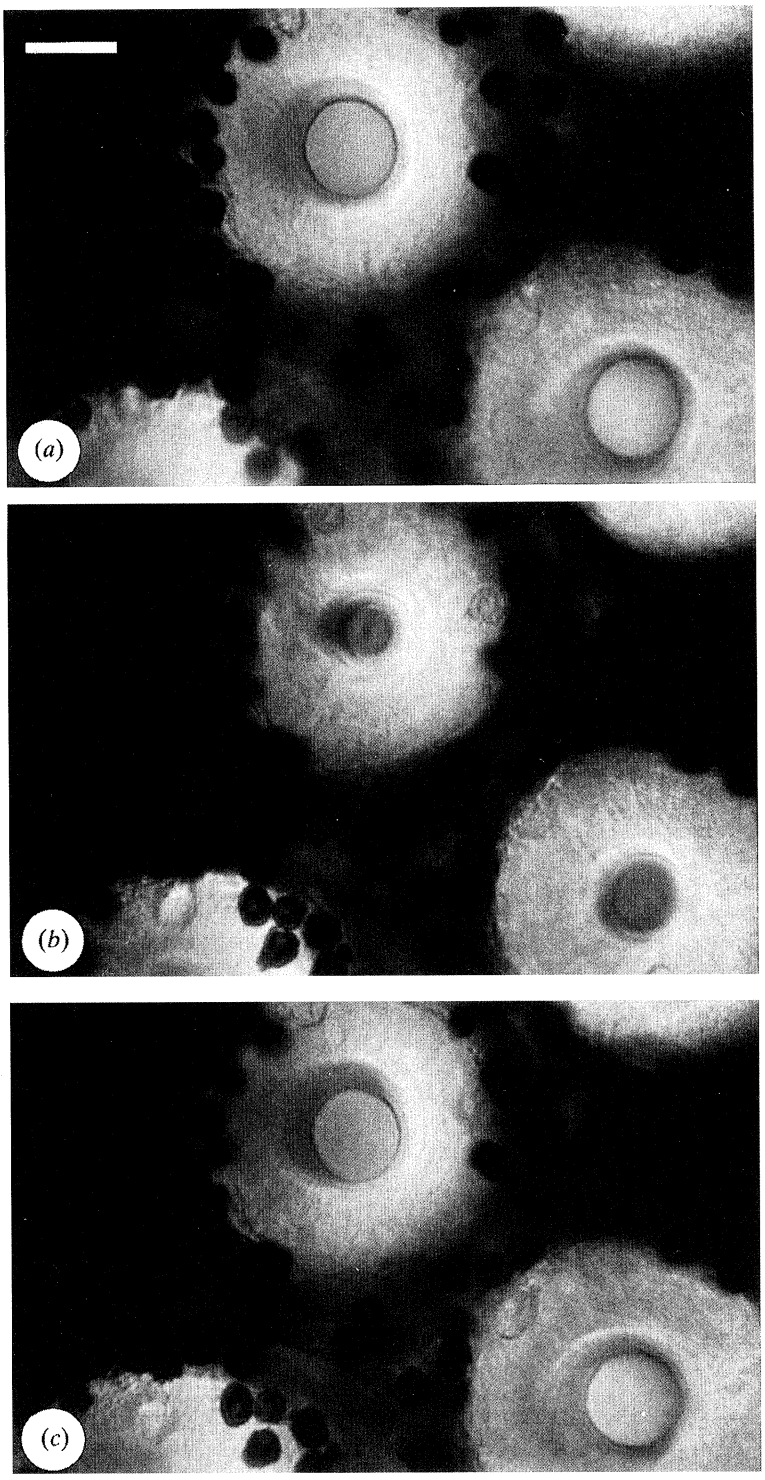

Figure 3. Changes in diameter of two external openings of the madreporite induced by ACh. (*a*) In ASW before the application of 10^{-5} M ACh. (*b*) Six mins after the immersion in ACh. (*c*) The recovery, 5 mins after the onset of wash with ASW. The dark round spots surrounding the pores are chromatophores. Bar represents 20 μm.

times the particles formed larger clumps. The water movement was studied by applying the carbon suspension near one end of the tube through a glass micropipette attached to a micromanipulator. Observation and recording were made with an inverted differential interference contrast microscope (TMD-NT, Nikon) fitted with a CCD (charge-coupled device) camera (Matsushita WV-BD400) and a video cassette recorder (Matsushita NV-G50). The experiments were carried out at room temperature (17–21 °C).

(*f*) *Rhodamine-phalloidin staining*

We examined whether the pore-canal cells contain F-actin by rhodamine-phalloidin staining. For this purpose, the soft tissue of the madreporite was separated from the ossicle, fixed and embedded in a polyester wax (BDH Ltd). The procedure for separating the soft tissue from the ossicle was the same as described above. It was then immersed in ASW containing 1 % dimethyl sulfoxide. The tissue was fixed

for 45–60 mins with 3.7% formaldehyde in ASW at room temperature or in a fixation buffer consisting of 75 mM KCl, 2 mM $MgCl_2$, 10 mM EGTA, 100 mM lysine, 320 mM sucrose and 25 mM piperazine-N-N′-bis(2-ethanesulfonic acid) (pH 6.8) (Bonder *et al.* 1989) at 4 °C. The fixed tissue was then rinsed in ASW or the buffer, dehydrated with a graded series of ethanol and embedded in polyester wax. The tissue was sectioned at 5–7 μm, rehydrated with a series of ethanol and immersed in a phosphate-buffered saline (PBS) containing rhodamine-phalloidin (Molecular Probes Inc.) at a concentration of 20–40 units per ml for 30–90 mins. Control sections were first incubated with the PBS containing excess (70 mM) non-labelled phalloidin (Sigma Chemical Co.) before labelling with the fluorescent probe. The sections were mounted in 80% glycerol under a coverslip after the excess label was rinsed twice with the PBS. The sections were observed with an epifluorescent microscope (EFD2, Nikon).

3. RESULTS

(*a*) *General observation of the external openings of the madreporite*

The madreporite occupies one of the five genital plates surrounding the anus. Figure 1 shows outside (aboral) views of a 'cleaned' madreporic ossicle of *Hemicentrotus pulcherrimus* observed with a SEM. There are about 380 pores in this madreporite which was obtained from an animal 2.8 cm in ambital diameter. The large hole indicated with an arrow in figure 1*a* is one of the genital openings. The plate also bears a few small spines. A spine base is indicated by an arrowhead in figure 1*a*.

A remarkable feature of the madreporic ossicle is the uniformity of its pores, which measure about 70 μm in diameter (figure 1*b*). The regularity of the pore size is also found in other species examined (*Pseudocentrotus depressus*, *Anthocidaris crassispina* and *Temnopleurus toreumaticus*). The inner walls of the pores are intricately perforated, giving them a lace-like appearance (figure 1*b*).

A very different view was obtained when the soft tissue of a fresh, unfixed and uncoated madreporite was observed with a low-vacuum SEM (WS-250, 'WET-SEM', Topcon Ltd). Unlike the pores of the 'cleaned' madreporic endoskeleton, the external openings of the soft tissue had variable diameters (figure 2). The diameter of the largest opening was about 40 μm. Similar variation in the pore size was also observed in *Pseudocentrotus depressus*. This indicates the possibility that the opening of each pore can change its diameter.

To observe the external openings of a live madreporite, water-immersion lenses were useful when they were used with transmitted light. The clearest image of the outline of the pore was obtained when we observed the thin piece of tissue sliced off the external surface of the madreporite. Figure 3*a* shows two external openings of a live madreporite. We could observe cilia beating inside the madreporic pores. To determine the direction of beating of the cilia, we observed the movement of particles (diameter > 1 μm) suspended in seawater near the outer surface of the madreporite. The particles never entered the pore of the isolated madreporite. Many chromatophores were seen in the aboral epithelial tissue among the external openings of the madreporite (figure 3). There was little spontaneous change of the pore size during our observation.

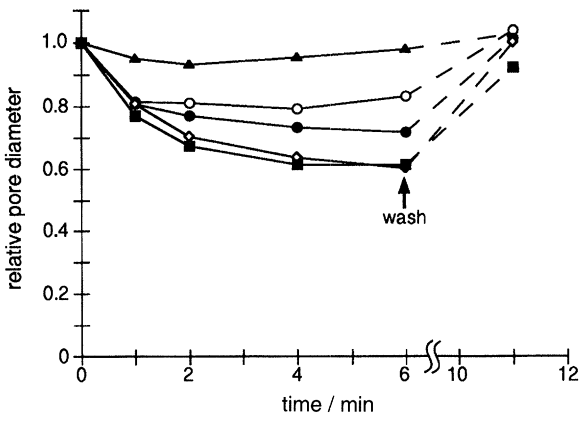

Figure 4. The relation between the time after the perfusion of ASW containing ACh and the relative pore diameter of the external openings of the madreporite. The diameter of each pore was normalized to the value before the perfusion of ACh. ACh was washed away after 6 mins' immersion by perfusing ASW for 1 min. The number of the animals used in the measurement is 3 for each concentration of ACh. The relative pore diameters are given as mean values. The standard deviation of each point varies from 0.02 (at 10^{-7} M, 2 min) to 0.17 (at 10^{-8} M, 6 min). The following symbols are used to represent different ACh concentration: 10^{-9} M (filled triangle), 10^{-8} M (open circle), 10^{-7} M (filled circle), 10^{-6} M (open diamond) and 10^{-5} M (filled square).

(*b*) *Pore constriction induced by chemical stimulation*

To see whether the pore size changes in response to stimulation, we studied the effects of ACh, Adr and a high concentration of K^+ on the isolated madreporite. When ASW containing ACh was perfused, the diameter of the external openings of the madreporite decreased. Figure 3 shows a typical response to 10^{-5} M ACh. The changes in diameter of the openings are plotted against time in figure 4 for five different concentrations of ACh. The lowest effective concentration of ACh was 10^{-8} M. Higher concentrations of ACh induced stronger responses, reaching a maximum at 10^{-6} M. Complete closure of the pore was not seen in our observation. The pore became most constricted (to about 60% of the initial diameter) 4 mins after the application of 10^{-5}–10^{-6} M ACh (figure 4). The mean pore diameter for the unstimulated madreporite was 20.9 μm (s.d. = 1.6 μm, $n = 6$), which decreased to 12.6 μm (s.d. = 1.9 μm, $n = 6$) 6 mins after the application of 10^{-5} M ACh. The response was reversible; when the ACh was washed away with ASW, the constricted pores regained their initial size in 5 mins.

To understand the nature of the response to ACh, we studied the effect of ACh-antagonists, atropine and *d*-TC. The antagonists were given 5 mins before the application of ACh. Atropine inhibited the pore closure

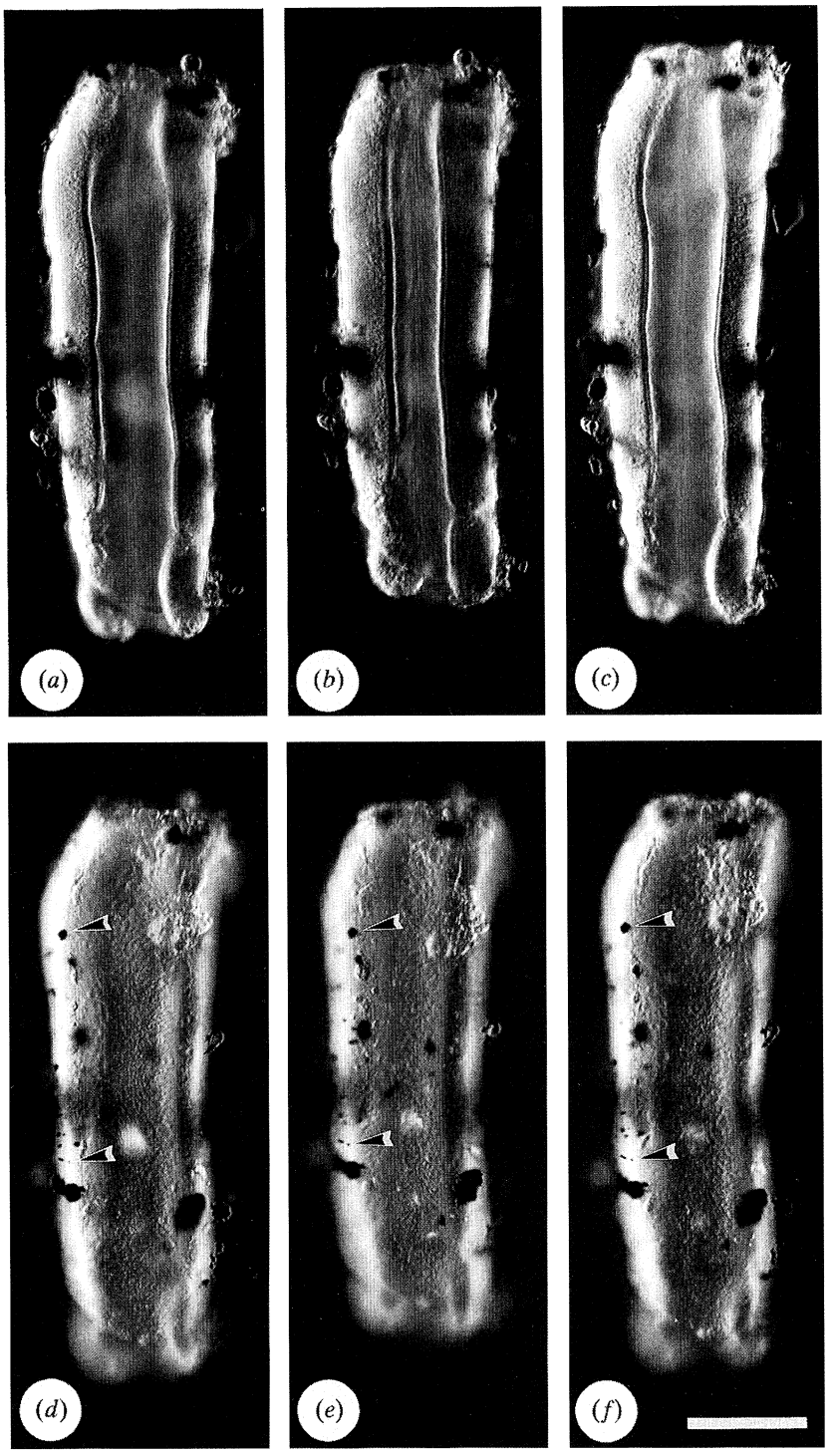

Figure 5. Effects of 10^{-5} M ACh on an isolated single pore tube observed under a differential interference microscope. The aboral (external) opening of the pore is at the top of the tube. The left column (*a*, *d*) shows the tube before the ACh treatment. The middle column (*b*, *e*) shows the tube 5 mins after the perfusion of ACh. The right column (*c*, *f*) shows the recovered state after 10 mins (three washes with ASW). Upper row: focused on the lumen; lower row: focused on the attached carbon particles (arrowheads). Bar represents 50 μm.

response induced by ACh reversibly. When the concentration of atropine was 10^{-4} M, the response to 10^{-8} M–10^{-6} M ACh was completely inhibited. The response to 10^{-5} M ACh was not completely inhibited but was reduced by 10^{-4} M atropine. The effect of various concentrations of atropine on the response to 10^{-7} M ACh was also studied. The lowest effective concentration of atropine was 10^{-5} M. Higher concentrations of atropine induced a stronger inhibition of the pore closure response, causing a complete inhibition at 10^{-4} M. Atropine alone did not change the pore size over the range of concentrations used in these experiments. *d*-TC (10^{-4} M) did not inhibit the pore closure response induced by 10^{-7} M ACh.

A pore closure response similar to that induced by ACh was also observed when the madreporite was perfused with ASW containing a high concentration of K^+ (320 mM NaCl, 150 mM KCl, 7 mM $CaCl_2$, 40 mM

Table 1. *Effect of ACh on the size of single pore tubes*

	inner diameter	outer diameter	height of 'collar'	height of cell		
	μm	μm	μm	μm	relative length	relative volume
Before ACh treatment	32.3±3.3	65.1+2.7	1.7±0.4	14.7±1.0	1.000	1.000
ACh-treated tube (10^{-5} M, 5 min)	22.3±3.1[c]	62.5±2.3[a]	2.1±0.4	18.2±1.5[b]	0.917±0.042[a]	0.983±0.088
after three washes (10 min)	30.4±2.1	64.6±2.6	1.8±0.5	15.1±0.8	0.999±0.074	0.979±0.099

(Inner diameter and height of cell parameters exclude the 'collar'. All values are mean±s.d., $n = 6$. [abc] denote significantly different results from both before treatment and after washes.)
[a] $p < 0.05$.
[b] $p < 0.01$.
[c] $p < 0.001$.

$MgCl_2$, 7 mM Tris; pH 8.0). Adr at 10^{-5} M had no effect on the pore diameter. The perfusion of any of the above solutions did not stop the activity of the cilia in the pore canal. Even when the pores became narrower, the cilia were still moving in the narrowed lumen of the pore canal.

Similar results were obtained in isolated madreporites that have not been sliced off, although precise measurement was difficult due to the poor optical conditions.

(*c*) *Morphology and responses of isolated pore tubes*

Figure 5*a* shows an isolated single pore tube observed under the differential interference microscope. The lumen of the tube is densely covered with cilia which beat continuously. All the cilia point their tips in the aboral direction. We could not observe the movement of individual cilia because of the dense ciliation in the tube. The inner-most part of the wall of the tube has an optical contrast different from that of the rest of the cells. This layer probably corresponds to the 'collars' observed by transmission electron microscopy (see the next section).

When 10^{-5} M ACh was perfused, the inner diameter of the tube decreased while the thickness of its wall increased (compare figure 5*a* with 5*b*). The decrease of the inner diameter of the tube was not restricted to the proximity of the external opening of the tube but was observed throughout the tube. The cilia in the constricted pore were still moving in the narrowed canal, pointing aborally as before. The response was reversible; both the inner diameter and the thickness of the cell wall resumed their original values after the removal of ACh (figure 5*a–c*).

Because a pore tube constitutes the lining of a cylindrical canal through the ossicle, we thought it highly probable that the pore closure response was associated with an increase in the volume of its cells. To see if this was the case, we determined the volumes of normal and constricted pore tubes by measuring their diameters and lengths.

To determine the effect of ACh on the tube length, carbon particles were attached to the outside of the tube. As shown in figure 5*d–f*, ACh induced a reversible shortening of the tube. The diameters of the tube were measured at fixed positions of the isolated single pore tube before and 5 mins after the application of 10^{-5} M ACh, and 10 mins after the removal of ACh by three washes with ASW. We measured both the inner and outer diameters, the height of the 'collar' and the thickness of the wall of the tube. Both the inner diameter and the thickness of the wall do not include the height of the 'collar'. We found that ACh reduced not only the inner diameter but also the outer diameter of the tube (table 1). The change in the height of the 'collar' was not significant ($p > 0.05$).

To see if a volume change is involved in the pore closure response, we made the following calculations. For this purpose, the outer diameter and the thickness of the wall were measured at two positions separated by a distance of 10 or 20 μm along the tube and the volume of the tube was calculated between these positions. The calculated volume does not include that of the 'collar'. We assumed that the tube was rotationally symmetrical around the midline of the pore canal and that both the outer diameter and the thickness of the wall change linearly between the two positions. The volume of the 10- or 20-μm long tube thus calculated was corrected for the length change measured by using the carbon particles. After this, the volume of the tube was normalized to the control (table 1). The results indicate that the cells lining the pore canal do not change their volume when the pore becomes narrower in response to ACh.

We also used isolated pore tubes to study the water movement in the pore canal. When Indian ink was applied through a micropipette near the aboral end of the tube, the ink was carried to the oral end through the pore canal. This was confirmed in 11 out of 15 trials made on 13 tubes. In these cases, the ink seemed to enter the tube from the edge of its aboral opening. In a tube shown in figure 6, the ink reached its oral end 8 s after it was applied near the aboral end. When we applied the ink near the oral end of a tube, the ink never entered the tube but was swept away from the oral end (observation were made on eight tubes). In some cases, however, although there was no bulk flow of ink through the pore, some large carbon particles (diameter > 1 μm) were observed to move to the

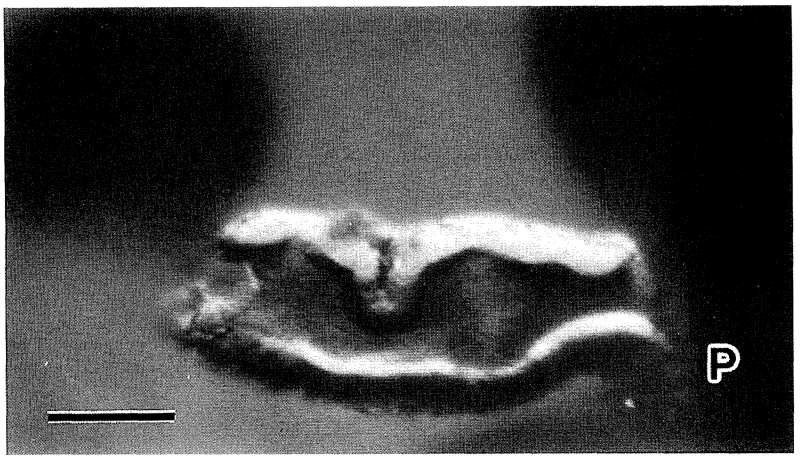

Figure 6. Water movement through a pore tube. A video frame showing Indian ink coming out of the oral end of the tube (left side) 30 s after it was applied from a micropipette (P) near the aboral opening. Bar represents 50 μm.

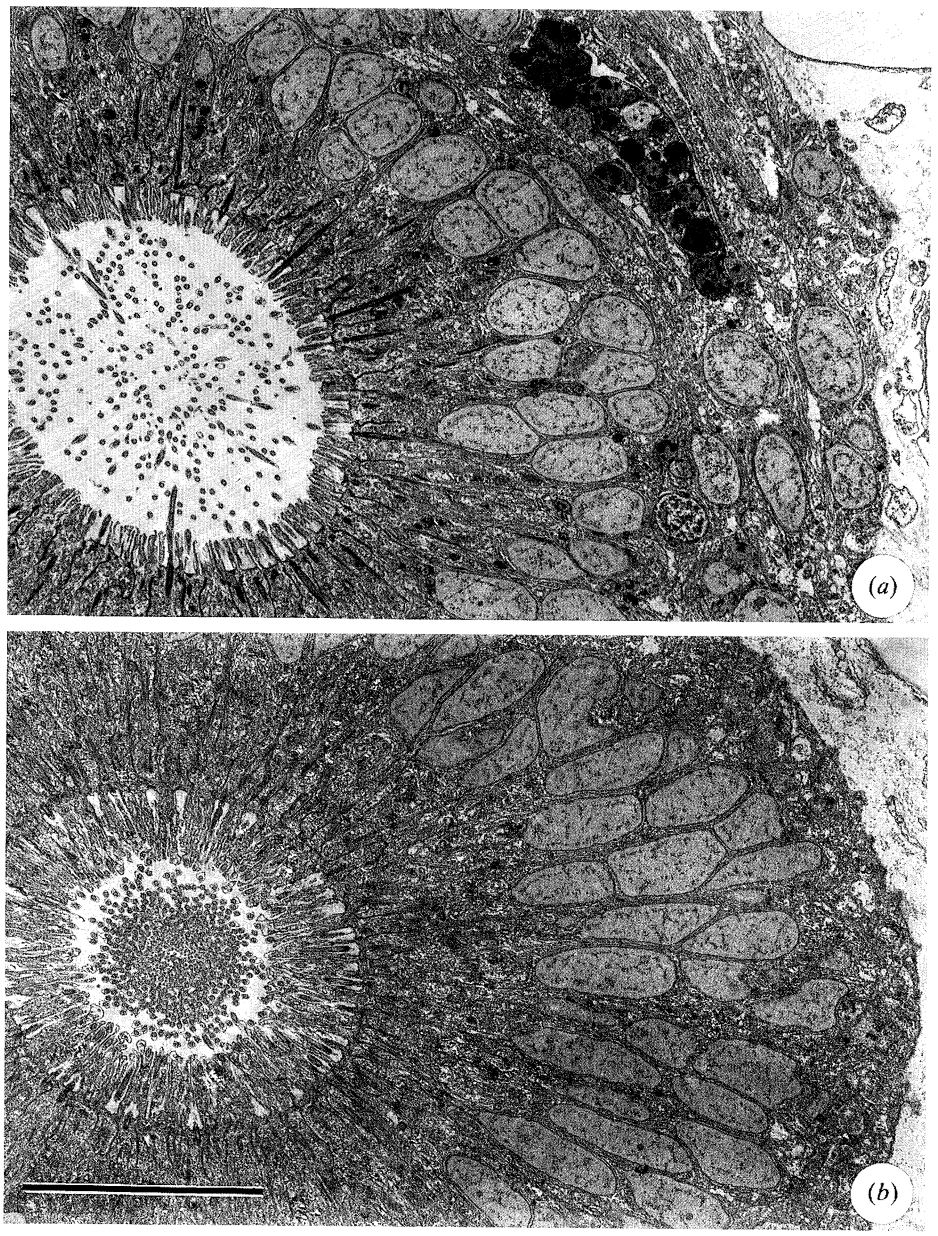

Figure 7. Transmission electron micrographs showing horizontal (transverse) sections of: (*a*) a pore canal fixed without a CCh treatment; and (*b*) a pore canal fixed after a CCh treatment. Bar represents 10 μm.

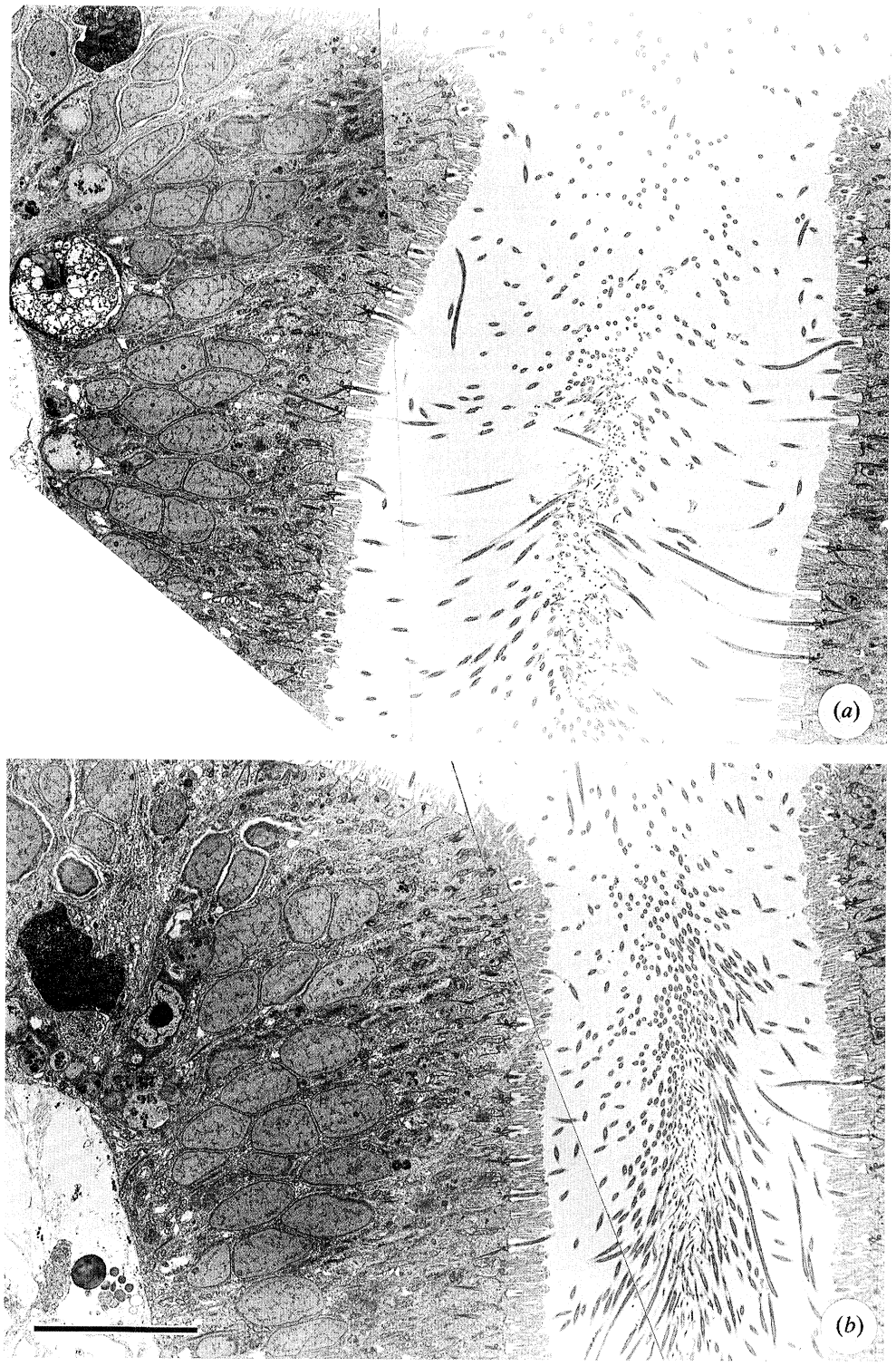

Figure 8. Transmission electron micrographs of vertical sections of: (*a*) a pore canal fixed without a CCh treatment; and (*b*) a pore canal fixed after a CCh treatment. Bar represents 10 μm.

aboral end. These particles were transported along the midline of the pore and were discharged from the aboral opening.

When Indian ink was applied to either the aboral (five trials) or the oral (four trials) end of tubes that had been constricted by 10^{-5} M ACh, the ink never reached the opposite end through the pore canal. On the other hand, large carbon particles that had entered the tube from its oral end were driven to the aboral end as in the normal tube.

(*d*) *Fine structure*

General views of horizontal (transverse) sections of pore canals fixed in both normal (not treated with CCh) and constricted (treated with CCh before fixation) states are shown in figure 7, and those of the vertical (axial) sections are shown in figure 8. The diameter of the lumen was smaller and the cells were taller in the CCh-treated than in the untreated specimens. In the constricted pore canal, the cilia were

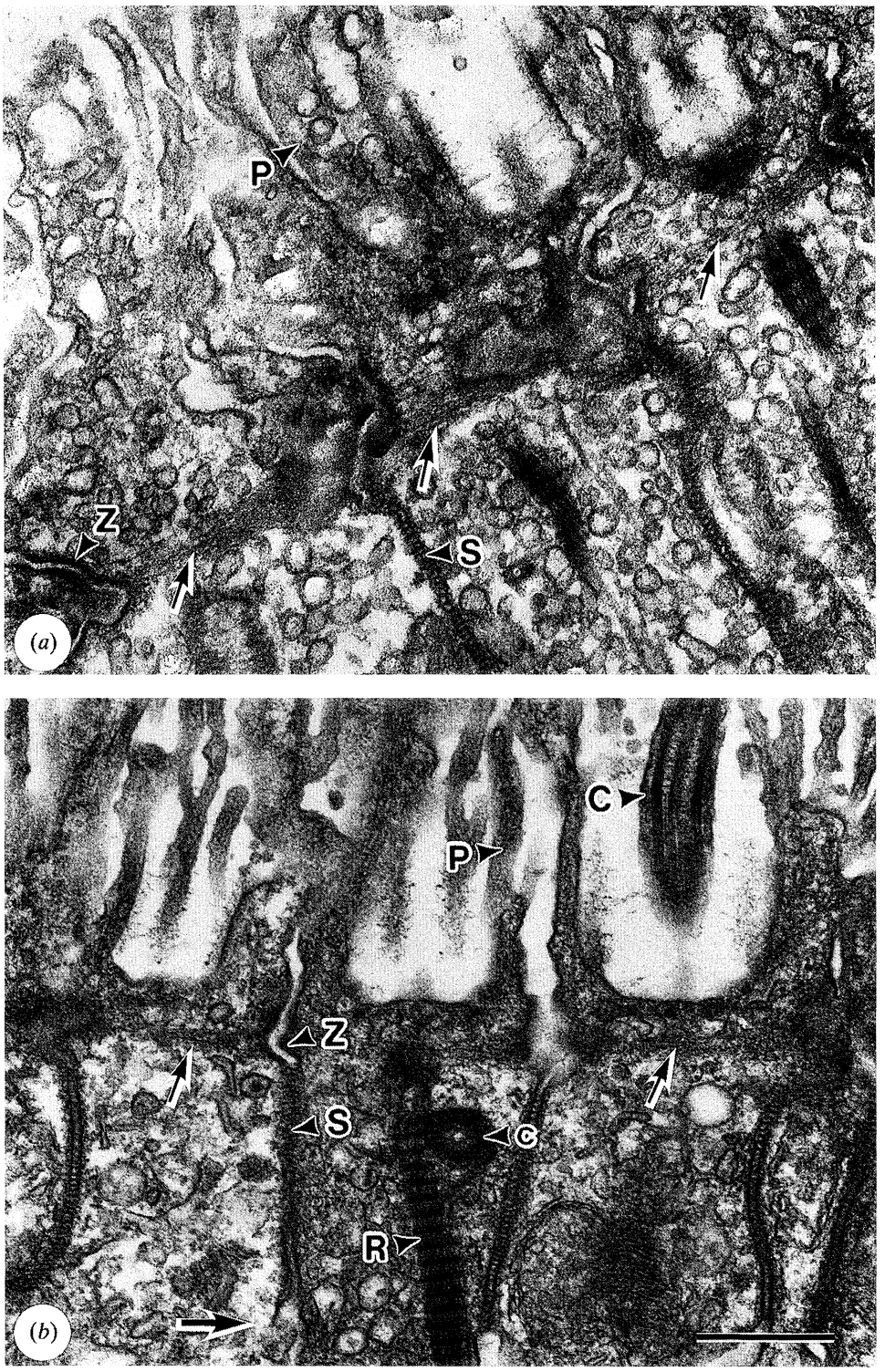

Figure 9. Transmission electron micrographs of apical regions of cells lining the lumen of the pore canal. (*a*) Horizontal section. (*b*) Vertical section. The smaller arrows indicate the filaments linking the adherens junctions. The larger arrow in (*b*) indicates the direction of the outer (aboral) surface. P: collar-like projection of the cell. S: septate junction. Z: adherens junction (*zonula adherens*). C: cilium. R: ciliary rootlet. c: centriole. Bar represents 0.5 μm.

densely packed in the centre of the lumen of the canal. The cilia were less closely packed in the CCh-untreated pore. The pore tubes generally consist of a single layer of columnar epithelial cells each bearing a single cilium on its luminal surface. The cilium is associated with a basal body, a centriole, a striated side-arm (not shown) and two striated ciliary rootlets (figure 9). The centriole is always on the aboral side of the basal body. The side-arm is located on the oral side. Because the water moves inwards in the lumen of the isolated pore tube (see the preceding section), the centriole is located in the opposite direction of the water movement with respect to the basal body. The proximal portion of the cilium is surrounded by a collar-like projection of the cell body (figures 7, 8, 9, 11). The pore canal cells thus resemble some ciliated cells of echinoderms (Nørrevang

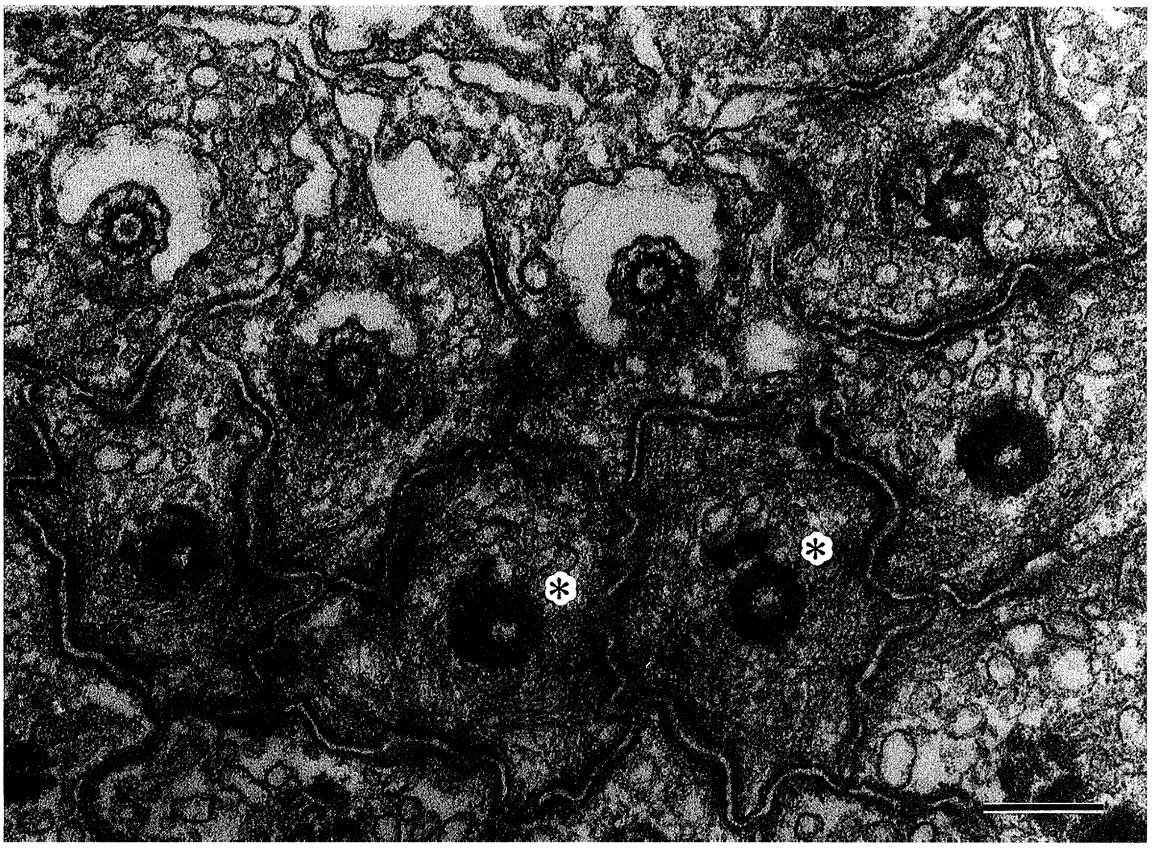

Figure 10. Transverse section of the pore-canal cells near their apical surface. Note the filaments circularly running just beneath the adherens junctions (e.g. in the cells marked with *). Bar represents 0.5 μm.

& Wingstrand 1970; Rehkämper & Welsch 1988; Martinez *et al.* 1991). As shown in figures 7 and 8, the height of the 'collar' appeared to be larger in the CCh-treated specimens than that in the untreated specimens. We measured the heights of the 'collars' of both the CCh-treated and untreated pores. The mean height of the 'collar' of the CCh-untreated pores was 1.2 μm (s.d. = 0.6 μm, $n = 43$) and that of the CCh-treated pores was 1.7 μm (s.d. = 0.4 μm, $n = 27$). The *t*-test indicates that their mean difference was significant ($p < 0.001$). But the increase in the height of the 'collar' alone cannot account for the closure of the pore. This is because the distance between the bases of the 'collars' on the opposing sides of the pore (inner diameter including the thickness of the 'collars') of the CCh-treated pore (15.8 ± 2.8 μm; mean ± s.d., $n = 27$) was significantly smaller ($p < 0.001$) than that of the untreated pore (21.5 ± 3.9 μm; mean ± s.d., $n = 43$).

In the apical region, the pore-canal cells are connected to each other by adherens junctions, and at the more basal region, by septate junctions (figures 9, 10) as in other echinoderm epithelial cells (Holland 1984). No cell junction was observed near the basal region of the pore canal. There are numerous clear vesicles in the 'collar' as well as in the apical part of the cell (figures 9–11). The basal two-thirds of the pore-canal cell are occupied by nuclei. At the base the pore-canal cells rest on a thin basal lamina (figure 12).

There are what look like cell processes between the pore-canal cell and the basal lamina. The processes sometimes form a cluster (figure 12) which may be a bundle of nerve fibres or processes of pore-canal cells. We found cellular profiles containing clear vesicles near the base of the pore-canal tissue throughout our study. These may be nerve endings. There seems to be few, if any, nerve endings in the pore-canal tissue. In fixed material there is a small space between the ossicle and the pore-canal tissue. The space appears to contain some extracellular material and a few cells. The external (aboral) surface of the madreporite is covered with epithelial cells that possess microvilli (figure 8). Unlike the 'collar' of the cells lining the pore canal, the middle portion of these microvilli appears to be associated with some extracellular material or cuticle, as in some epidermal cell surface of other echinoderms (Holland 1984). Ciliation was sparse on the external surface of the madreporite.

No muscle cells were found in or near the pore-canal tissue. At the apical region of each cell, many filaments were found apparently linking the adherens junctions. (figures 9, 10). The filaments were found both in the CCh-treated and untreated specimens. Filaments were also found in the basal region of some cells (figure 13). The filaments form a thick bundle and run parallel to the long axis of the cell. A schematic drawing of a pore-canal cell is shown in figure 14.

(*e*) *Rhodamine-phalloidin staining*

A cross section of pore canals stained with rhodamine-phalloidin is shown in figure 15*a*. Strong fluorescence was observed near the lumen of the pore

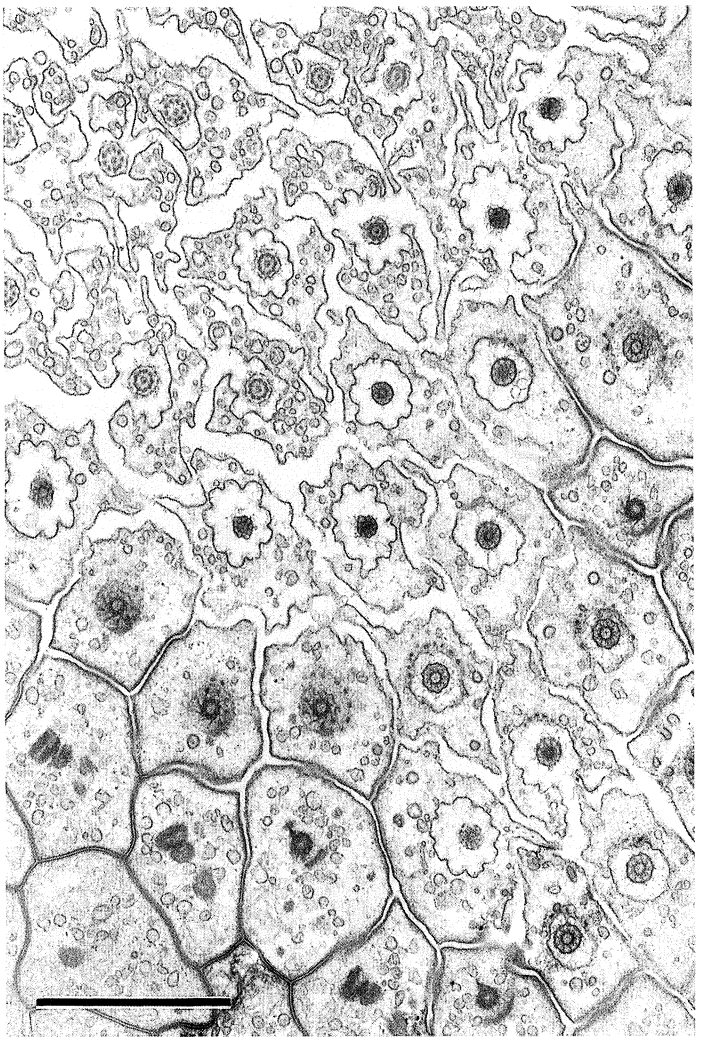

Figure 11. Tangential section of the luminal wall. A collar-like projection of the pore-canal cell surrounds the base of each cilium. Bar represents 2 μm.

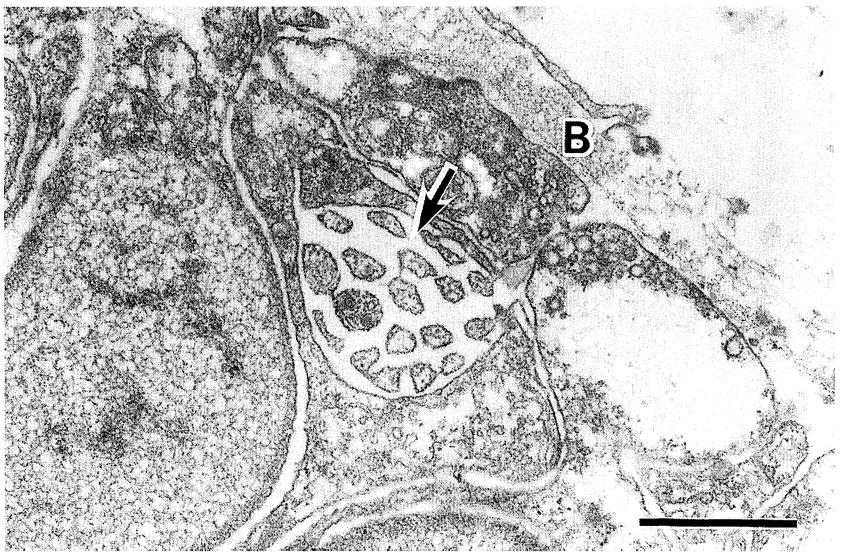

Figure 12. Horizontal section near the base of the pore canal showing the clusters of cell processes (arrow) between the pore-canal cell and the basal lamina (B). These processes are possibly a bundle of nerve fibres. Bar represents 1 μm.

canal. The inner-most part of the strongly labelled region seems to be composed of fine projections pointing towards the centre of the lumen and to correspond to the 'collar' of the pore-canal cell. Adjacent and basal to this part, the labels were found running circularly around the lumen of the pore. This

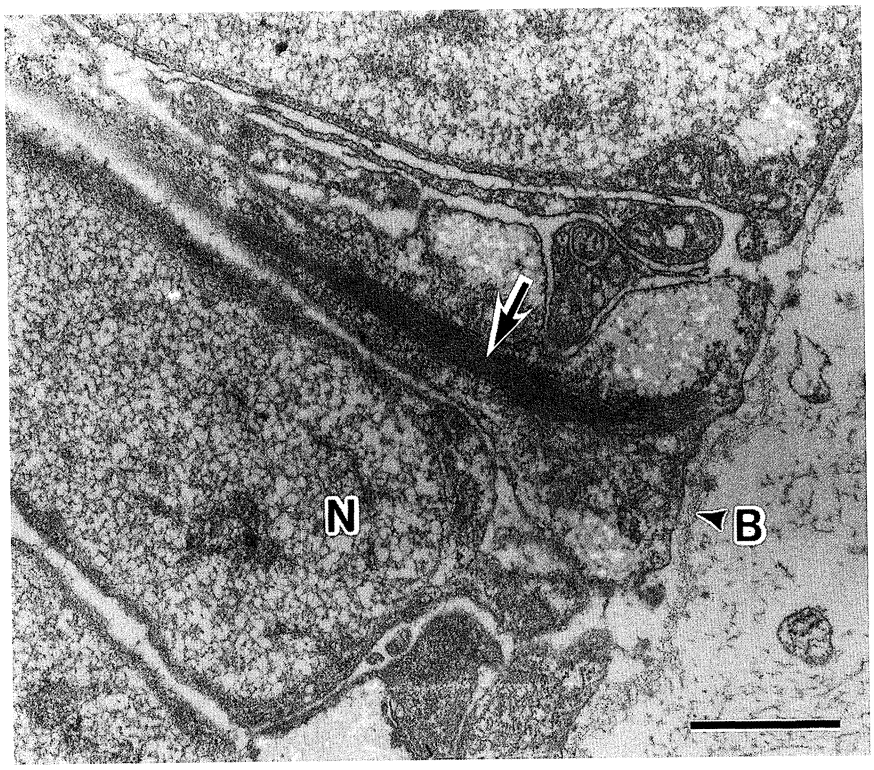

Figure 13. Vertical section at the base of the pore canal showing a bundle of filaments (arrow). B: basal lamina. N: nucleus. Bar represents 1 μm.

region seems to correspond to the apical part of the pore-canal cell where filaments were found by TEM. A tangential section of the epithelium lining a pore canal is shown in figure 16. The region that seems to be near the luminal surface of the epithelium appears to be divided into many blocks by the fluorescent label. Each block seems to correspond to the apical part of a cell. Little fluorescence was observed in the control sections treated with excess non-labelled phalloidin before staining.

4. DISCUSSION

(*a*) *The pore closure response*

Our study has shown that the external openings of the madreporite reversibly narrow in response to stimulation. To our knowledge, the only other report on a similar response is that of Ferguson (1988) who mentions that closure of the madreporic pores occurs in an asteroid. As will be discussed later, our finding will give a clue to understanding the function of the madreporite.

We will, however, first discuss the mechanism of the pore closure response itself. Broadly, there are two possible mechanisms for the pore closure response: cell swelling and contraction.

Calculations based on the measurements of the isolated single pore tubes suggest that the cells lining the pore canal do not change their volume when the pore changes its diameter. It is therefore likely that the pore closure response is brought about by a contractile mechanism without an associated volume change.

As no muscle or sphincter-like cells were found in the pore tube, some contractile structure other than muscle seems to be involved in the pore constriction. For the contractile structure to constrict the pore, its most strategic location would be either near the lumen of the pore or near the outer boundary of the pore tube. Few filaments were found in the basal region of the pore-canal cell. In contrast, filaments were found in the apical region of each pore-canal cell, apparently associated with the adherens junctions. Staining with rhodamine-phalloidin suggested that the filaments are composed of F-actin. It is possible that the apical region of the cell contracts by an interaction of actin and myosin to induce the pore closure response. Ferguson & Walker (1991) found filament bundles in the apical region of the pore-canal cell of the madreporite of asteroids and suggested their possible contractile role in the pore constriction.

Filament bundles similar to those observed in the pore-canal cells have been reported in various organs of other animals. In the morphogenesis of some organs, such as the neural tube formation of vertebrates, it is suggested that the filaments encircling the apical region of each cell consist of actin and that their contraction causes apical constriction of the cell (Hilfer & Searls 1986). Also, in the apical region of the epithelial cells of the small intestine of some vertebrates, it is suggested that filaments linking the adherens junctions consist of actin and that the filaments cause apical constriction of the cell through their interaction with myosin (Hirokawa *et al.* 1982, 1983).

If the pore closure response is caused by contraction of the filament bundles while the cell volume is kept constant, we would expect changes in the dimensions of the pore tube other than those described above, that is,

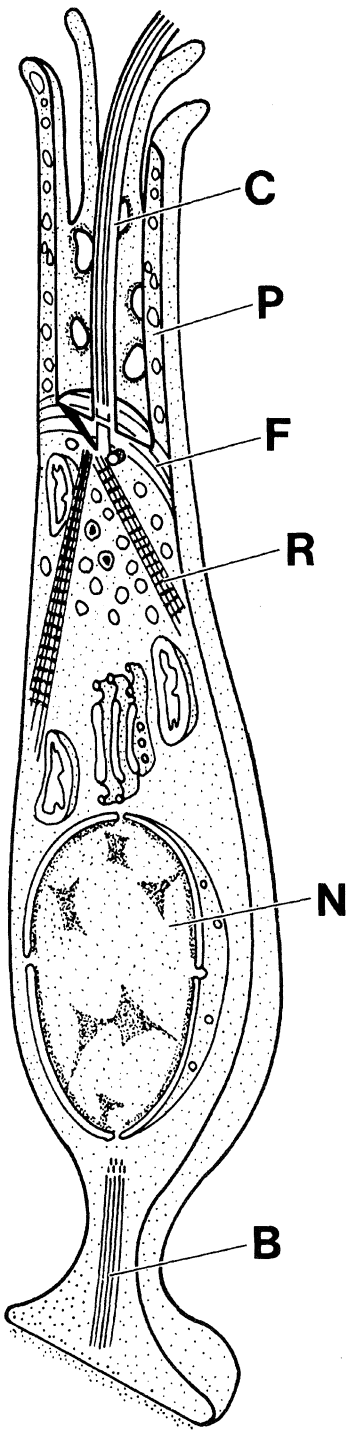

Figure 14. Schematic drawing of a pore-canal cell. B: bundle of filaments. C: cilium. F: actin-like filaments. N: nucleus. P: collar-like projection. R: ciliary rootlet.

shortening of the pore tube and/or decrease of its outer diameter. Both changes were observed in the isolated single pore tubes: the outer diameter decreased by 2.6 μm and the length was reduced by 8% when the inner diameter of the tube decreased from 32.3 μm to 22.3 μm (table 1). It is possible that the decrease of the outer diameter occurs only in the isolated pore tube because the pore tube is a lining of a cylindrical hole through the rigid ossicle. If the outer diameter cannot change, the relative length of the tube should become 0.85 when the inner diameter is reduced to 22.3 μm. However, a decrease in outer diameter of the pore tube is possible if tissue fluid in the space between the tube and the mesh-like ossicle is replenished from other tissue spaces.

If a contractile structure near the lumen of the pore is responsible for the pore constriction, it should shorten by up to 20% of its length per minute because the inner diameter is reduced by up to 20% per min (figure 4). This value seems very slow in comparison with the shortening velocity of invertebrate smooth muscle. For example, the longitudinal muscle of a holothurian, *Isostichopus badionotus* shortens at 0.44 muscle length per second (2640% per min) at 24–27 °C (Tsuchiya 1985). The rate of the constriction of the pore is comparable to that of the contractile ring. For example, in the first cleavage of a sea urchin egg, the contractile ring shortens at the rate of 14% per min (Ishikawa & Noguchi 1988). The results obtained with the isolated pore tube as well as with TEM suggest that the pore closure response is caused by a shortening of fibre bundles in the apical region of the pore-canal cell.

On the inner surface of the pore canal, there are collar-like projections surrounding the proximal region of cilia. TEM observations showed that these 'collars' are longer in the constricted (CCh-treated) pore than in the normal (CCh-untreated) pore. Although the measurements made on isolated single pore tubes failed to detect a significant change in the 'collars' during the pore closure response, probably because of the difficulty in determining the lengths of the short (1–2 μm) 'collars', we assume that the 'collars' lengthen in the pore closure response. The increase in the height of the 'collars' alone, however, cannot account for the closure of the pore (see Results). The elongation may be caused by an elevation of the internal pressure of the pore-canal cell due to the contraction of the filaments in the apical region of the cell. There are filaments in the 'collars' which may contain F-actin as suggested by rhodamine-phalloidin staining. These filaments may be involved in the elongation of the 'collars'. The elongated 'collars' in the constricted pore, together with the closely packed cilia in the lumen of the pore canal, seem to function as a stopper (see also the next section).

ACh (and its analogue, CCh) and a high concentration of K^+ caused the pore closure response. ACh is known to induce contraction in echinoderm muscles (Welsh 1966) and to change the stiffness of catch connective tissues of echinoderms (Takahashi 1967; Motokawa 1981, 1983). Physiological and morphological evidence suggests that a cholinergic nervous control is involved in the contraction of the echinoderm muscles (Welsh 1966; Pentreath & Cobb 1972; Florey & Cahill 1980). Cholinergic nervous control may also be involved in the response of the catch connective tissues. The effects of ACh, atropine and *d*-TC on the tissue obtained from the aboral surface of the madreporite suggest that its pore size may also be under a cholinergic (probably muscarinic) control. Adr does not seem to be involved in the control of the pore size. The result that a high K^+ solution induced a pore closure response suggests that a membrane depolarization is involved in the pore closure response.

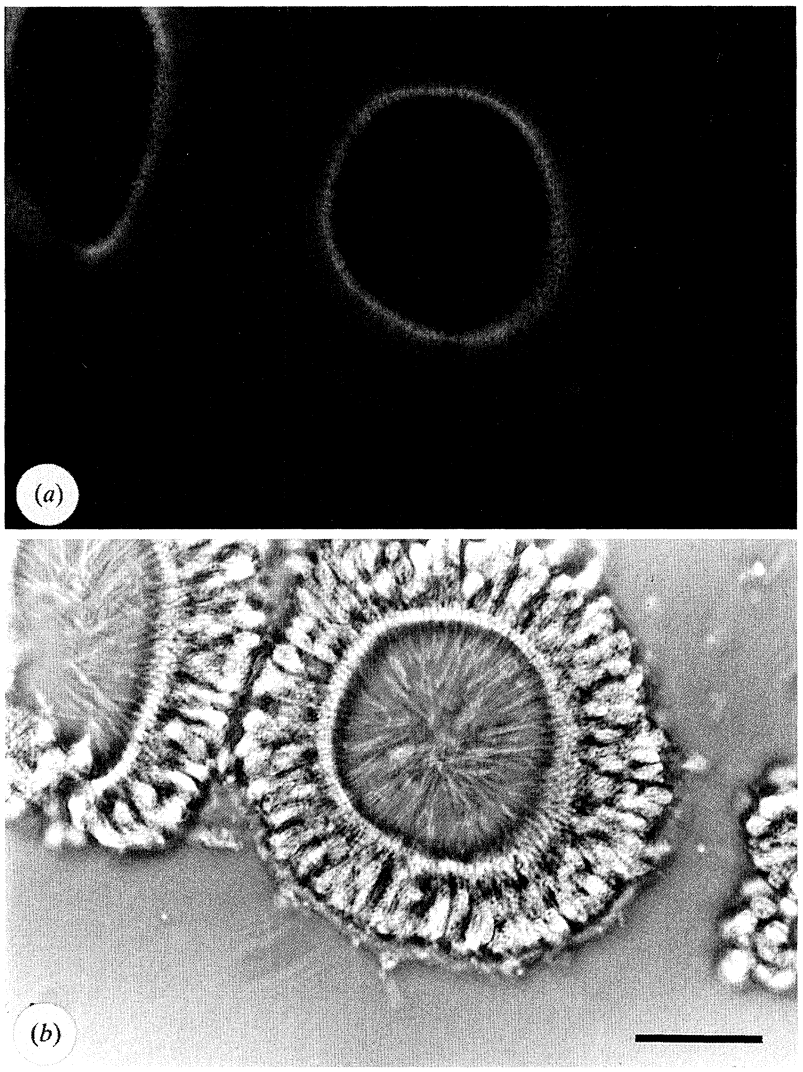

Figure 15. A cross section of pore canals stained with rhodamine-phalloidin. (*a*) Fluorescent light micrograph. (*b*) Phase contrast micrograph. Bar represents 20 μm.

(*b*) *Function of the madreporite*

To understand the function of the madreporite, it is essential to know whether there is a water flow across it and, if there is one, in which direction the flow occurs. There have been many studies on the nature of water movement through the madreporite, but no consistent results have been obtained. Thus, some investigators reported that the water moves outwards across the madreporite and the larval pore canal (Hartog 1887; Ruppert & Balser 1986) whereas others reported that it moves inwards (Ludwig 1890; MacBride 1896; Gemmill 1914; Budington 1942; Bargmann & Behrens 1964; Ferguson 1984, 1988, 1989, 1990, 1992). Fechter (1965) reported that there is essentially no water movement across the madreporite and put forward a hypothesis that the madreporite serves as a pressure equalizer between the outside and the inside of the water-vascular system. Ellers & Telford (1992) questioned this hypothesis arguing that the madreporite could function as a pressure equalizer only when there is an air bubble in the body cavity of the sea urchin.

Our study using Indian ink has shown that the fluid flows through the isolated pore tube in the oral direction which corresponds to the inward flow in the intact animal. We have also found that larger particles (> 1 μm) are transported along the midline of the pore in the opposite direction, that is, from the oral end to the aboral end of the isolated pore tube. Apparently similar observation has been made by Bamber (1921) in the stone canal of *Echinus* where there is a peripheral inward current and a central outward current. There is thus bidirectional transport through the pore, by which water is taken into the water-vascular system while large particles are carried outwards. The controversy about the water movement across the madreporite seems to have been due to the bidirectional nature of transport.

Ruppert & Balser (1986) observed the movement of latex microbeads in the hydropore of the asteroid larva. They concluded that there is an outward current in the pore canal and suggested that the madreporite functions as an excretory organ. Their conclusion may be wrong because the particle movement shows only one aspect of the bidirectional transport as shown by our study. Some authors have ascribed the inward flow through the pore canal to the action of cilia in the stone

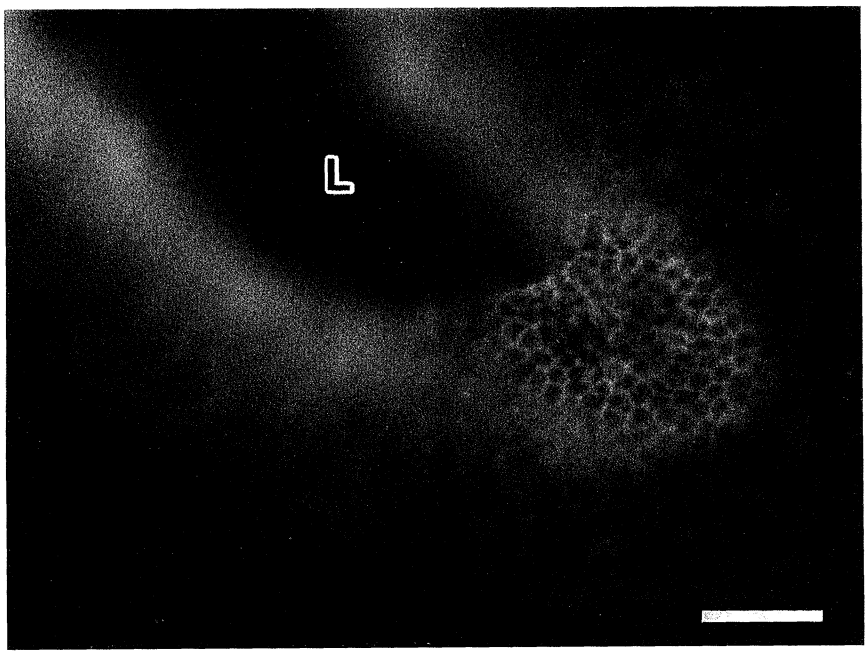

Figure 16. A fluorescent micrograph of a grazing section of a pore canal stained with rhodamine-phalloidin. The region near the luminal surface of the canal is found to be encircled by the fluorescent label and divided into many blocks. Each block seems to correspond to the apical part of each cell. The labelled region seems to correspond to the one where filaments are found by TEM. L: lumen of the pore canal. Bar represents 10 μm.

canal (Gemmill 1914; Budington 1942). Our study has, however, shown that the pore canal cilia themselves are capable of causing the inflow. Thus although a possibility of the excretory function (Welsch & Rehkämper 1987) cannot be ruled out, our results indicate that the madreporite is not a mere excretory organ.

Our result indicates that the centriole of the cilium is located in the opposite direction of the water movement with respect to the basal body. Apparently, this is contrary to Anstrom's observation on the ciliary basal apparatus of the blastula of *Lytechinus pictus* (Anstrom 1992). However, the bidirectional nature of ciliary transport observed in the pore tube makes it difficult to determine the direction of effective stroke from the direction of water flow alone. A further study on the ciliary activity in the madreporite is in progress.

It is most likely that the transport through the madreporite is regulated by the pore closure response. By changing its pore size, the madreporite may regulate the volume or the pressure of fluid in the water-vascular system. The pore may also close to prevent the entry of toxic substances into the water-vascular system. The stone canal may also participate in the regulation of fluid transport into and out of the water-vascular system. According to Rehkämper & Welsch (1988), there are muscle-like cells in the stone-canal tissue suggesting that the size of the lumen of the stone canal may change.

In our experiments, the pore did not close completely under any conditions. It is possible that the complete closure takes place under natural conditions, but it is also possible that the observed (incomplete) closure has nearly the same effect on the water flow as the complete closure. The central area of the constricted pore is filled with closely packed cilia (figure 7) which may function as a plug to obstruct the flow. To ascertain this possibility, we calculated the effect of the pore constriction on the flow rate through the pore canal shown in figure 7. We assumed that the pore is a true cylinder with a radius corresponding to the mean value of the longer and the shorter radii of the cross section because compression seems to have occurred at the sectioning. The radii of the pores thus calculated were 6.5 μm (open pore) and 4.2 μm (constricted pore). The cross section of the area occupied by closely packed cilia in the constricted pore was approximated by a true circle with a radius of 3.1 μm. According to Hagen-Poiseuille's law, the flow rate in the open pore tube (Q_o) is given by:

$$Q_o = [\Delta P \cdot \pi \cdot (6.5\ \mu\text{M})^4]/8L\eta,$$

where ΔP is the pressure difference between the two ends of the tube, L the length of the canal and h the coefficient of viscosity of seawater. The flow rate in the constricted pore tube (Q_c) is given by:

$$Q_c = \Delta P \cdot \pi \cdot \{[(4.2^4 - 3.1^4) - (4.2^2 - 3.1^2)^2 / \ln(4.2/3.1)]\ \mu\text{m}^4\}/8L\eta,$$

if the fluid cannot pass through the area where cilia are closely packed. Assuming that ΔP and L do not change, Q_c is 0.45% of Q_o. Without closely packed cilia,

$$Q'_c = [\Delta P \cdot \pi \cdot (4.2\ \mu\text{m})^4]/8L\eta,$$

which is 17% of Q_o. These calculations suggest the possibility that the cilia of the pore canal can function as a stopper in the constricted pore. Our observation on isolated single pore tubes supports this idea; Indian ink applied to one end of the constricted tube never reached the opposite end through the pore canal although the cilia pointed aborally and were still moving in the narrowed canal.

Our study has shown that water flows through the isolated pore tube in the oral direction, and that the water currents are regulated by the pore closure response which can completely block the flow. Constant influx of water does not seem to be necessary to maintain the hydraulic pressure in the water-vascular system because obstruction of the madreporite does not immediately impair the movement of the tube feet (Dakin 1923; Fechter 1965). Ferguson (1992) has reported that obstruction of the starfish madreporite, where a constant inflow seems to occur, does not impede the activity of the tube feet for 10 days. More detailed studies on the water movement in the intact animal seem necessary to understand the function of the madreporite.

Part of the work was carried out while M.T. and K.T. were at the Zoological Institute, University of Tokyo. Some of the experiments were done at the Misaki Marine Biological Station of the University of Tokyo (MMBS) and we thank Professor Masaaki Morisawa and the staff of the MMBS for the use of the facilities and for collecting the animals. We thank Mr. Ohki at the Research Cooperation Department, Tokyo Institute of Technology, for his help with the SEM, and we are indebted to the Topcon Ltd for the use of the 'WET-SEM'. Thanks also to Professor Yukihisa Hamaguchi for technical advice and for the use of the facilities. We are grateful to Dr J. C. Ferguson for valuable comments on the earlier version of the manuscript.

REFERENCES

Anstrom, J. A. 1992 Organization of the ciliary basal apparatus in embryonic cells of the sea urchin, *Lytechinus pictus*. *Cell Tiss. Res.* **269**, 305–313.

Bargmann, W. & Behrens, Br. 1964 Über die Tiedemannschen Organe des Seesterns. *Z. Zellforsch.* **63**, 120–133.

Bamber, R. C. 1921 Note on some experiments on the water vascular system of *Echinus*. *Proc. Liverpool Biol. Soc.* **35**, 64–70.

Binyon, J. 1964 On the mode of functioning of the water vascular system of *Asterias rubens* L. *J. Mar. Biol. Ass. U.K.* **44**, 577–588.

Bonder, E. M., Fishking, D. J., Cotran, N. M. & Begg, D. A. 1989 The cortical actin-membrane cytoskeleton of unfertilized sea urchin eggs: analysis of the special organization and relationship of filamentous actin, nonfilamentous actin, and egg spectrin. *Devl Biol.* **134**, 327–341.

Budington, R. A. 1942 The ciliary transport system of *Asterias forbesi*. *Biol. Bull.* **83**, 438–450.

Dakin, W. J. 1923 Note on the function of the water-vascular system of echinoderms. *Proc. Liverpool Biol. Soc.* **37**, 70–73.

Dietrich, H. F. & Fontaine, A. R. 1975 A decalcification method for ultrastructure of echinoderm tissue. *Stain Technol.* **50**, 351–354.

Eakin, R. M. & Brandenburger, J. L. 1979 Effect of light on ocelli of seastars. *Zoomorphologie* **92**, 191–200.

Ellers, O. & Telford, M. 1992 Causes and consequences of fluctuating coelomic pressure in sea urchins. *Biol. Bull.* **182**, 424–434.

Fechter, H. 1965 Über die Funktion der Madreporenplatte der Echinoidea. *Z. vergl. Physiol.* **51**, 227–257.

Ferguson, J. C. 1984 Translocative functions of the enigmatic organs of starfish – the axial organ, hemal vessels, Tiedemann's bodies and rectal caeca: an autoradiographic study. *Biol. Bull.* **166**, 140–155.

Ferguson, J. C. 1988 Madreporite and anus function in fluid volume regulation of a starfish (*Echinaster graminicola*). In *Echinoderm biology* (ed. R. D. Burke, P. V. Mladenov, P. Lambert & R. L. Parsley), pp. 603–609. Rotterdam: A. A. Balkema.

Ferguson, J. C. 1989 Rate of water admission through the madreporite of a starfish. *J. exp. Biol.* **145**, 147–156.

Ferguson, J. C. 1990 Seawater inflow through the madreporite and internal body regions of a starfish (*Leptasterias hexactis*) as demonstrated with fluorescent microbeads. *J. exp. Zool.* **255**, 262–271.

Ferguson, J. C. 1992 The function of the madreporite in body fluid volume maintenance by an intertidal starfish, *Pisaster ochraceus*. *Biol. Bull.* **183**, 482–489.

Ferguson, J. C. & Walker, C. W. 1991 Cytology and function of the madreporite systems of the starfish *Henricia sanguinolenta* and *Asterias vulgaris*. *J. Morphol.* **210**, 1–11.

Florey, E. & Cahill, M. A. 1980 Cholinergic motor control of sea urchin tube feet: evidence for chemical transmission without synapses. *J. exp. Biol.* **88**, 281–292.

Gemmill, J. F. 1914 The development and certain points in the adult structure of the starfish *Asterias rubens* L. *Phil. Trans. R. Soc.* B **205**, 213–294.

Hartog, M. M. 1887 The true nature of the 'madreporic system' of Echinodermata, with remarks on nephridia. *Ann. Mag. Nat. Hist. Ser. 5* **20**, 321–326.

Hilfer, S. R. & Searls, R. L. 1986 Cytoskeletal dynamics in animal morphogenesis. In *Developmental biology; a comprehensive synthesis, vol. 2 The cellular basis of morphogenesis* (ed. L. W. Browder), pp. 3–29. New York, London: Plenum Press.

Hirokawa, N., Tilney, L. G., Fujiwara, K. & Heuser, J. E. 1982 Organization of actin, myosin, and intermediate filaments in the brush border of intestinal epithelial cells. *J. cell Biol.* **94**, 425–443.

Hirokawa, N., Keller, T. C. S. III, Chasan, R. & Moosker M. S. 1983 Mechanism of brush border contractility studied by the quick-freeze, deep-etch method. *J. cell Biol.* **96**, 1325–1336.

Holland, N. D. 1984 Echinodermata; Epidermal cells. In *Biology of the integument, vol. 1 Invertebrates* (ed. J. Breiter-Hahn, A. G. Matoltsy & K. S. Richards), pp. 756–774. Berlin, Heidelberg, New York, Tokyo: Springer-Verlag.

Ishikawa, M. & Noguchi, M. 1988 Echinoderms (4) Echinoidea. In *Experiments in development of marine invertebrate* (ed. M. Ishikawa & T. Numakunai), pp. 122–166. Tokyo: Baifukan. (In Japanese.)

Ludwig, H. 1890 Über die Function der Madreporenplatte und des Steinkanals der Echinodermen. *Zool. Anz.* **313**, 377–379.

MacBride, E. W. 1896 The development of *Asterina gibbosa*. *Quart. J. Microsc. Sci.* **38**, 339–411.

Martinez, A., Lopez, J., Villaro, A. C. & Sesma, P. 1991 Choanocyte-like cells in the digestive system of the starfish *Marthasterias glacialis* (Echinodermata). *J. Morphol.* **208**, 215–225.

Motokawa, T. 1981 The stiffness change of the holothurian dermis by chemical and electrical stimulation. *Comp. Biochem. Physiol.* C **70**, 41–48.

Motokawa, T. 1983 Mechanical properties and structure of the spine-joint central ligament of the sea urchin, *Diadema setosum* (Echinodermata, Echinoidea). *J. Zool.* **201**, 223–235.

Nichols, D. 1966 Functional morphology of the water-vascular system. In *Physiology of Echinodermata* (ed. R. A. Boolootian), pp. 219–244. New York: John Wiley.

Nørrevang, A. & Wingstrand, K. G. 1970 On the occurrence and structure of choanocyte-like cells in some echinoderms. *Acta Zool.* **51**, 249–270.

Pentreath, V. W. & Cobb, J. L. S. 1972 Neurobiology of echinodermata. *Biol. Rev.* **47**, 363–392.

Prusch, R. D. 1977 Solute secretion by the tube foot epithelium in the starfish *Asterias forbesi*. *J. exp. Biol.* **68**, 35–43.

Prusch, R. D. & Whoriskey, F. 1976 Maintenance of fluid volume in the starfish water vascular system. *Nature, Lond.* **262**, 577–578.

Rehkämper, G & Welsch, U. 1988 Functional morphology of the stone canal in the sea urchin *Eucidaris* (Echinodermata: Echinoidea). *Zool. J. Linn. Soc.* **94**, 259–269.

Ruppert, E. E. & Balser, E. J. 1986 Nephridia in the larvae of hemichordates and echinoderms. *Biol. Bull.* **171**, 188–196.

Shimakura, S. & Robinson, V. 1989 Observation of wet specimens by the scanning electron microscope. *Biseibutsu* **5**, 64–72. (In Japanese.)

Takahashi, K. 1967 The catch apparatus of the sea urchin spine II. Response to stimuli. *J. Fac. Sci. Univ. Tokyo IV* **11**, 109–120.

Takahashi, K. & Tamori, M. 1988 Changes in pore size of the echinoid madreporite induced by chemical stimulation. In *Echinoderm biology* (ed. R. D. Burke, P. V. Mladenov, P. Lambert & R. L. Parsley), p. 814. Rotterdam: A. A. Balkema.

Takahashi, K., Tamori, M., Shingyoji C. & Matsuno, A. 1991 Structure of the pore canal of the echinoid madreporite. In *Biology of Echinodermata* (ed. T. Yanagisawa, I. Yasumasu, C. Oguro, N. Suzuki. & T. Motokawa), p. 549. Rotterdam/Brookfield: A. A. Balkema.

Takahashi, K., Tamori, M., Shingyoji, C. & Murakami, A. 1987 Responses of the sea-urchin madreporite induced by chemical stimulation. *Doubutsu Seiri* **4**, 131.

Tamori, M., Shingyoji, C. & Takahashi, K. 1990 Acetylcholine-induced constriction of single pore canals isolated from the sea-urchin madreporite. *Hikaku Seiri Seikagaku* **7**, 212.

Tamori, M., Shingyoji, C. & Takahashi, K. 1991*a* Isolation of single pore canals from the sea-urchin madreporite. In *Biology of Echinodermata* (ed. T. Yanagisawa, I. Yasumasu, C. Oguro, N. Suzuki & T. Motokawa), p. 550. Rotterdam/Brookfield: A.A. Balkema.

Tamori, M., Matsuno, A. & Takahashi, K. 1991*b* An ultrastructural study of the echinoid madreporite with special reference to its pore-closure response. *Hikaku Seiri Seikagaku* **8**, 179.

Tamori, M., Matsuno, A. & Takahashi, K. 1991*c* Fine structure of the echinoid madreporite with special reference to its pore-closure response. *Zool. Sci.* **8**, 1057.

Tamori, M. & Takahashi, K. 1992 Actin-like filaments with a possible role in the pore-closure response of the echinoid madreporite. *Hikaku Seiri Seikagaku* **9**, 222.

Tsuchiya, T. 1985 The maximum shortening velocity of holothurian muscle and effects of tonicity change on it. *J. exp. Biol.* **119**, 31–40.

Venable, J. H. & Coggeshall, R. 1965 A simplified lead citrate stain for use in electron microscopy. *J. cell Biol.* **25**, 407–408.

Welsch, U. & Rehkämper, G. 1987 Podocytes in the axial organ of echinoderms. *J. Zool.* **213**, 45–50.

Welsh, J. H. 1966 Neurohumors and neurosecretion. In *Physiology of Echinodermata* (ed. R. A. Boolootian), pp. 545–560. New York: John Wiley.

(*Received 30 November 1995; accepted 20 December 1995*)

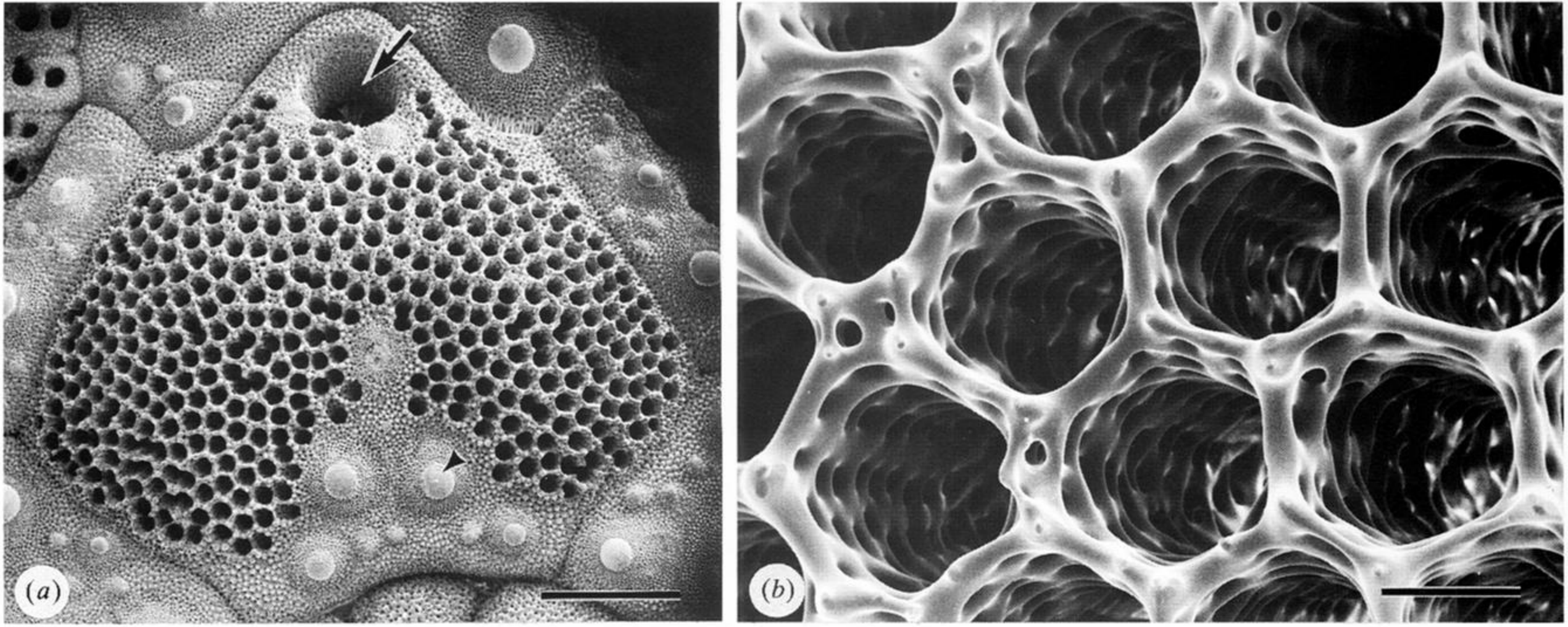

Figure 1. Outside (aboral) views of a madreporic ossicle of *Hemicentrotus pulcherrimus* (ambital diameter: 2.8 cm). (*a*) The whole ossicle: the arrow indicates the gonopore, the arrowhead indicates a spine base. Bar represents 500 μm. (*b*) A part of (*a*) at higher magnification. Bar represents 50 μm.

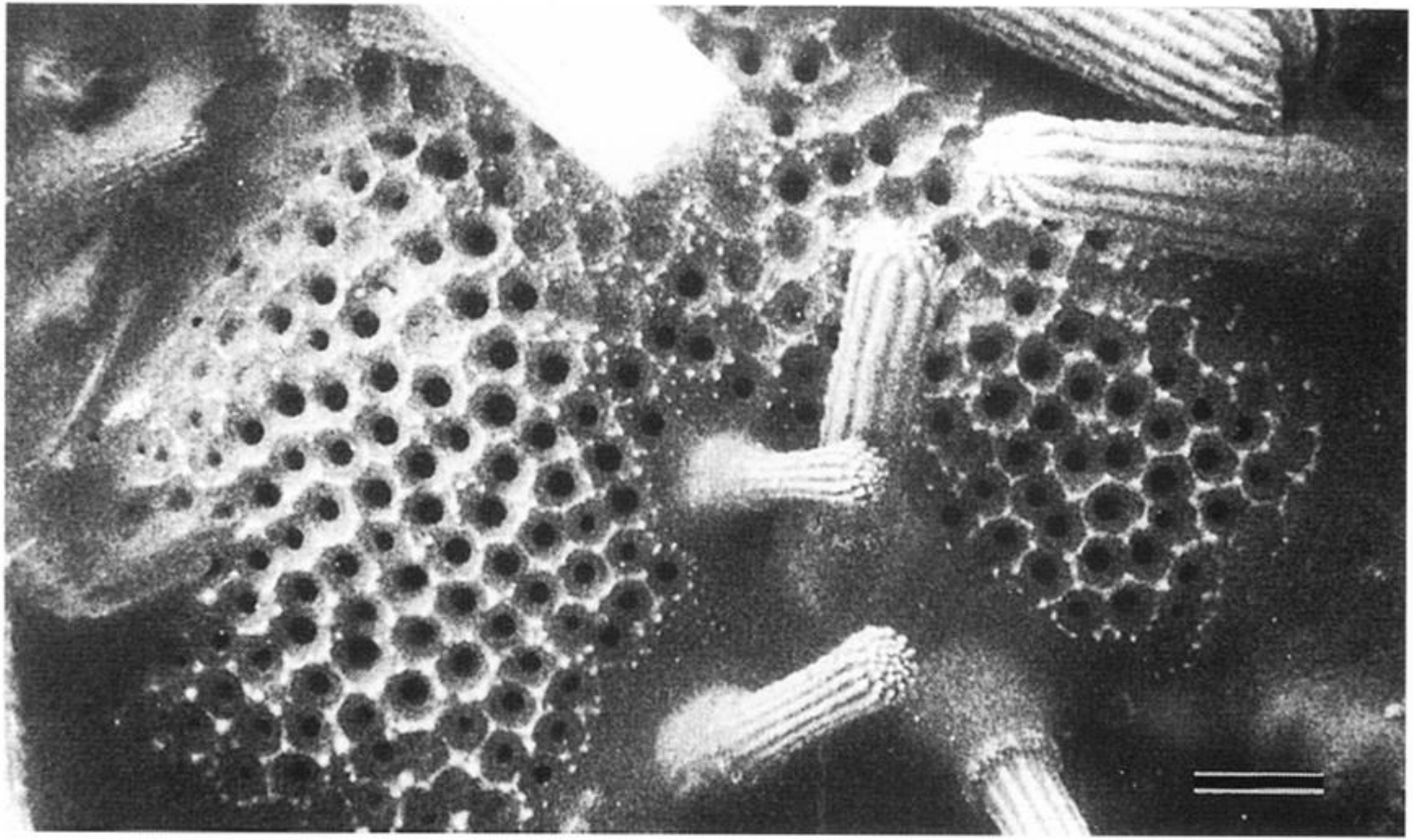

Figure 2. An outside (aboral) view of a fresh, unfixed and uncoated madreporite of *Hemicentrotus pulcherrimus* (ambital diameter: 2.2 cm) observed with a 'WET-SEM'. Bar represents 200 μm.

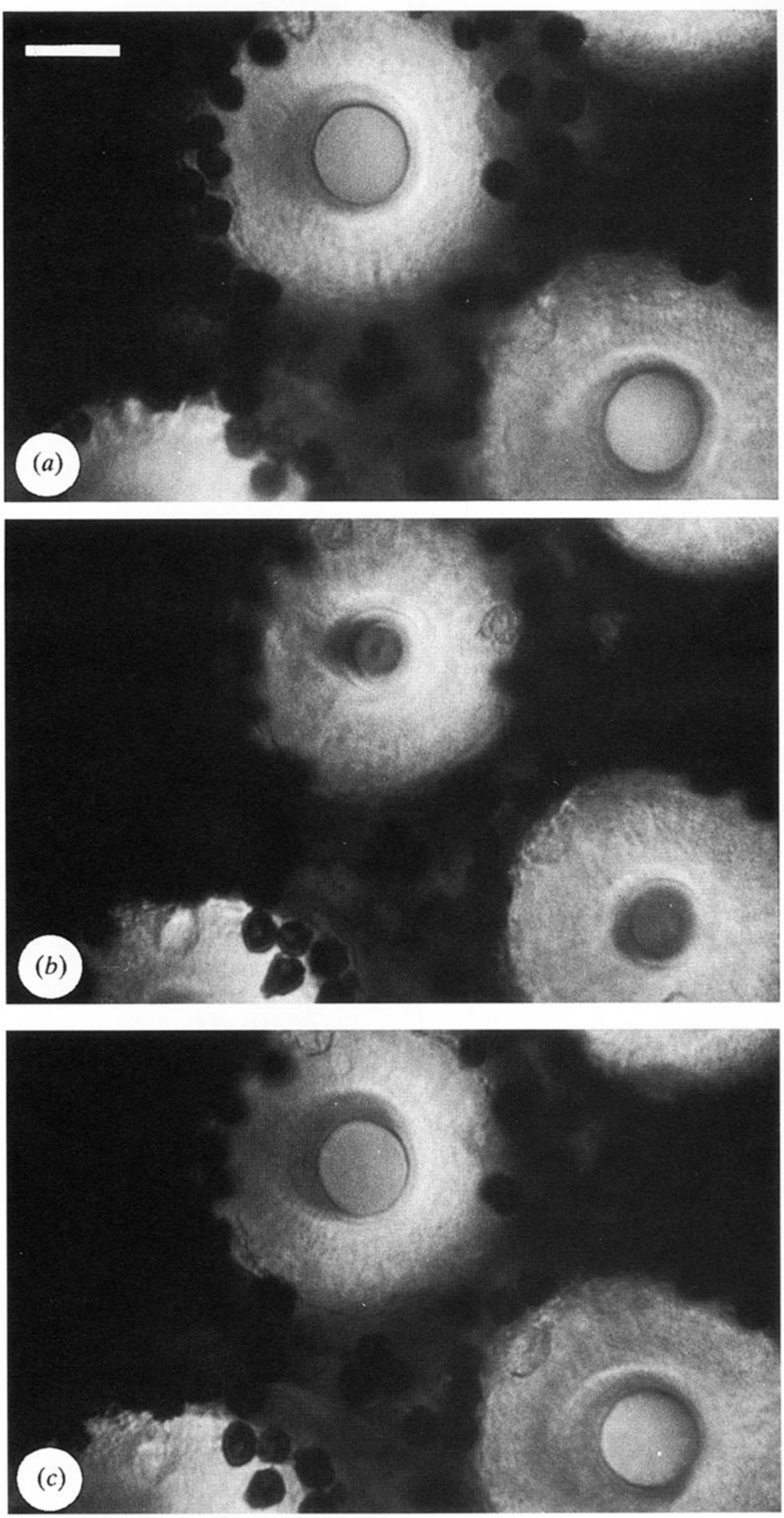

Figure 3. Changes in diameter of two external openings of the madreporite induced by ACh. (*a*) In ASW before the application of 10^{-5} M ACh. (*b*) Six mins after the immersion in ACh. (*c*) The recovery, 5 mins after the onset of wash with ASW. The dark round spots surrounding the pores are chromatophores. Bar represents 20 μm.

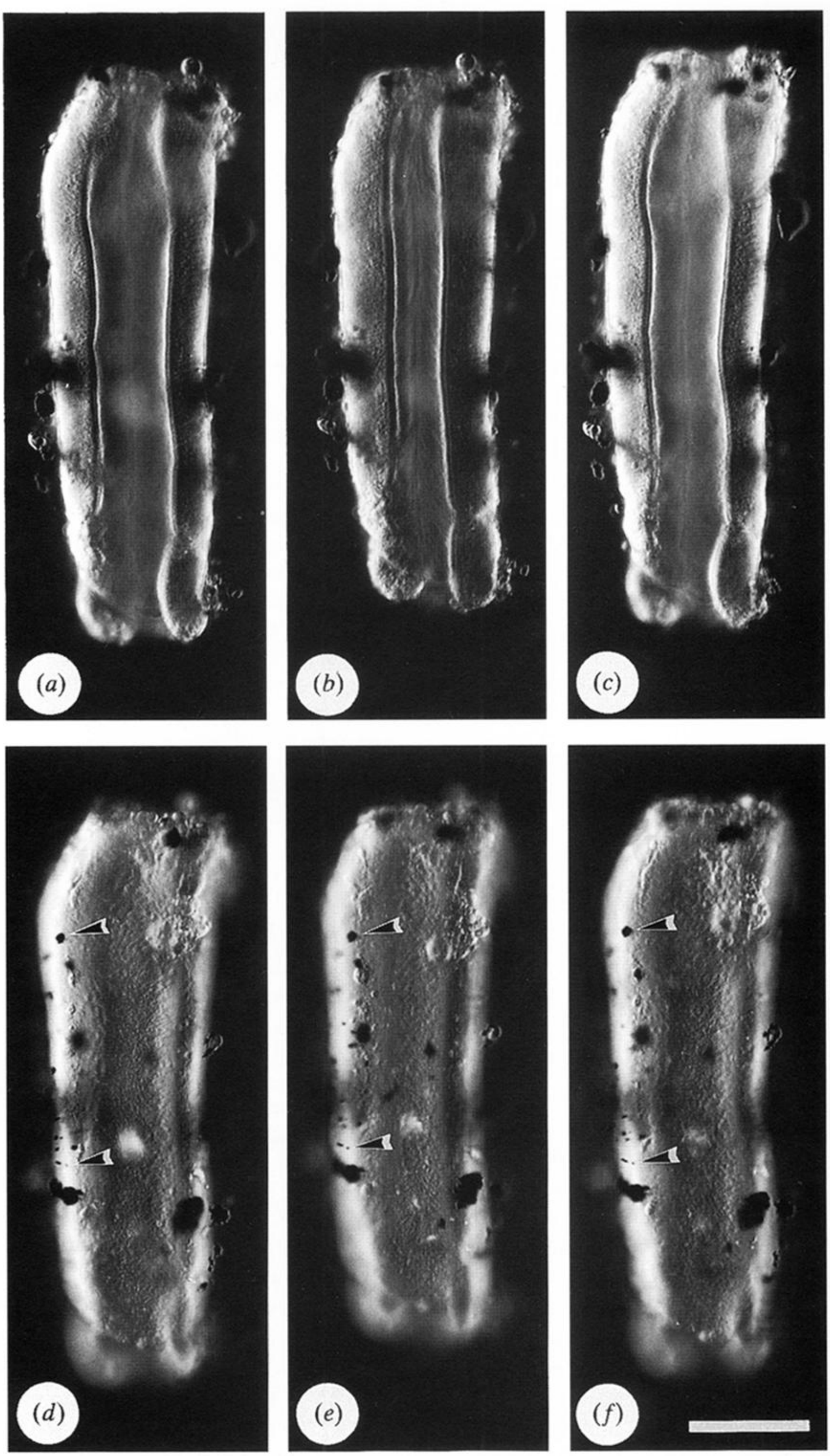

Figure 5. Effects of 10^{-5} M ACh on an isolated single pore tube observed under a differential interference microscope. The aboral (external) opening of the pore is at the top of the tube. The left column (*a*, *d*) shows the tube before the ACh treatment. The middle column (*b*, *e*) shows the tube 5 mins after the perfusion of ACh. The right column (*c*, *f*) shows the recovered state after 10 mins (three washes with ASW). Upper row: focused on the lumen; lower row: focused on the attached carbon particles (arrowheads). Bar represents 50 μm.

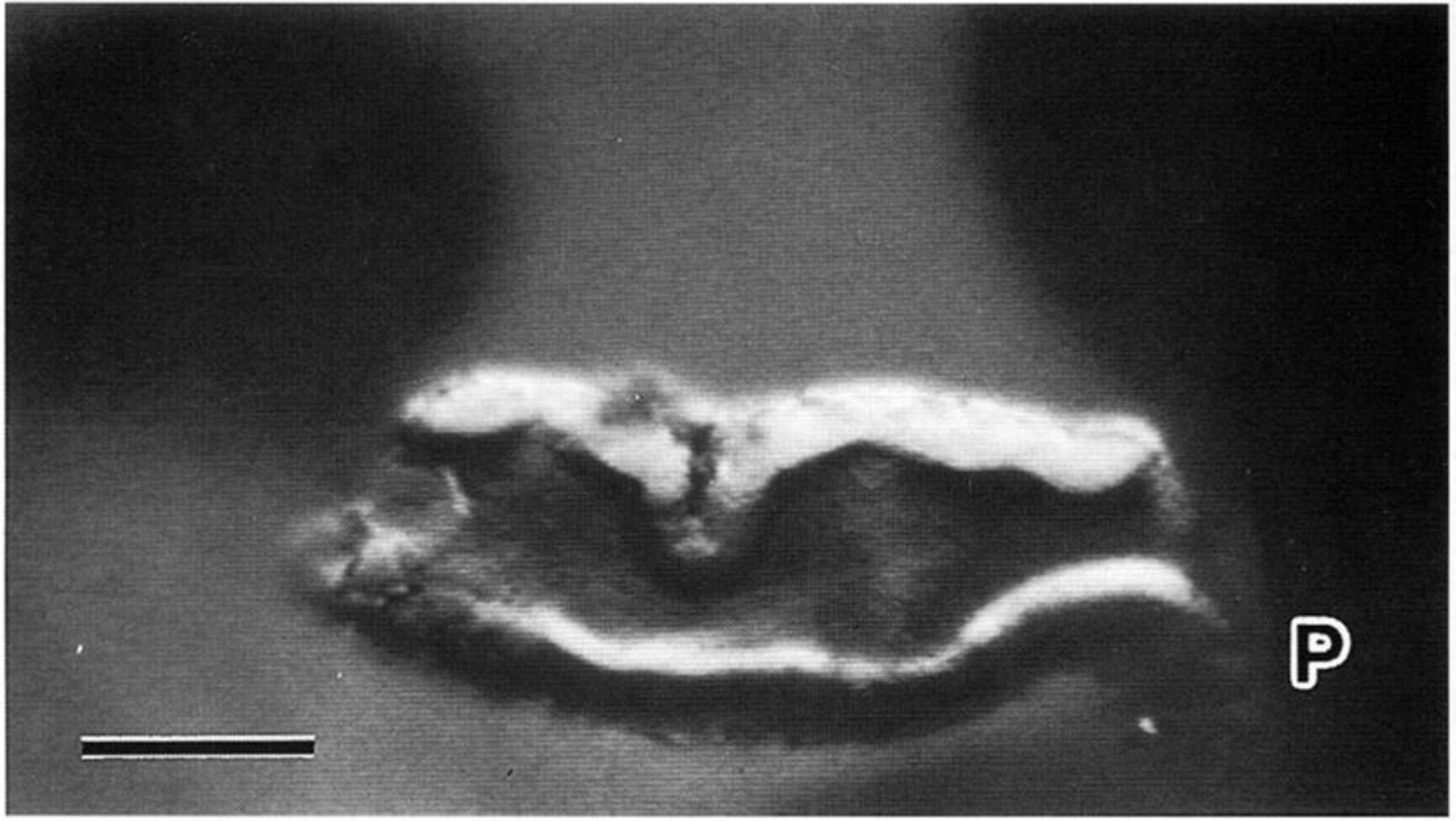

Figure 6. Water movement through a pore tube. A video frame showing Indian ink coming out of the oral end of the tube (left side) 30 s after it was applied from a micropipette (P) near the aboral opening. Bar represents 50 μm.

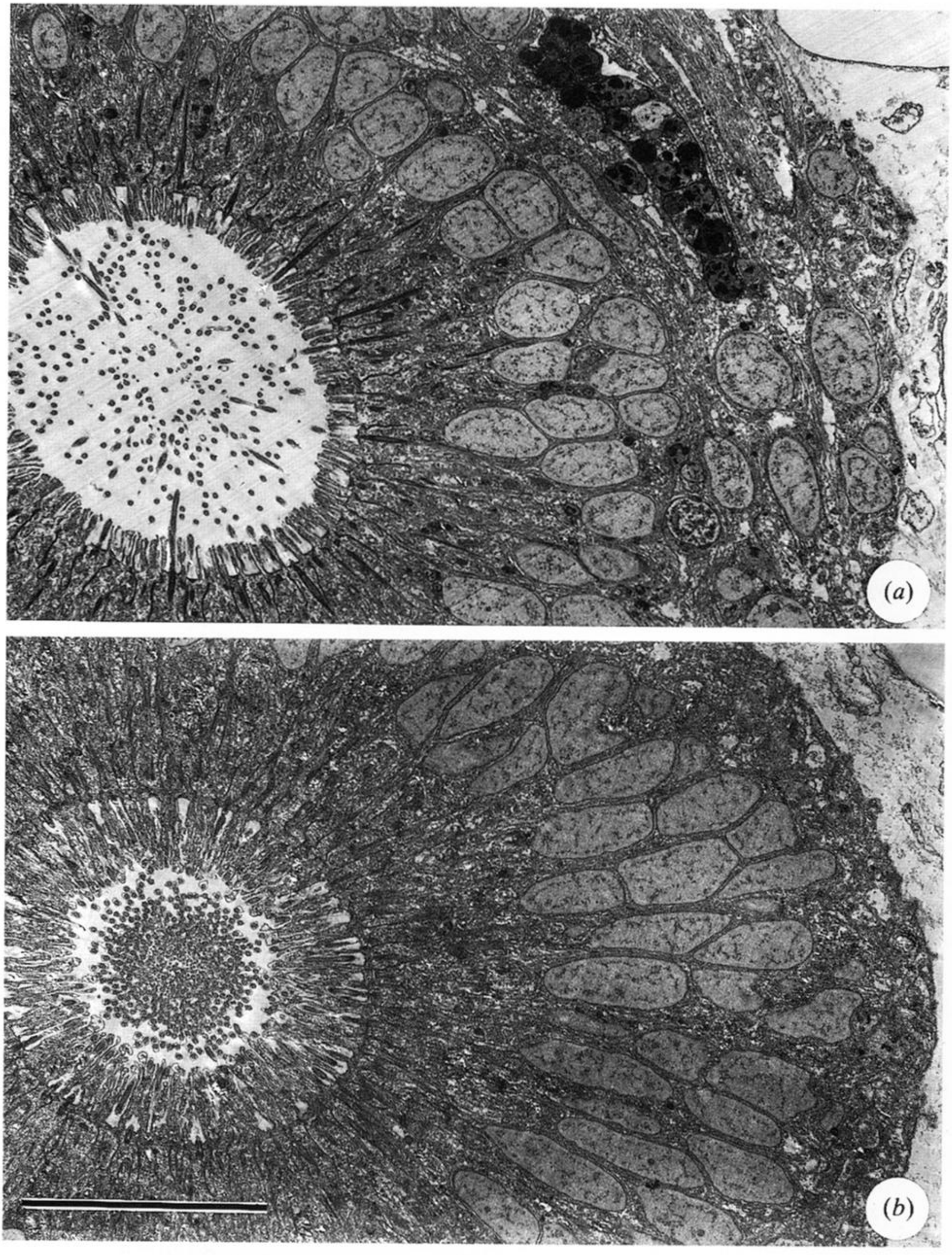

Figure 7. Transmission electron micrographs showing horizontal (transverse) sections of: (*a*) a pore canal fixed without a CCh treatment; and (*b*) a pore canal fixed after a CCh treatment. Bar represents 10 μm.

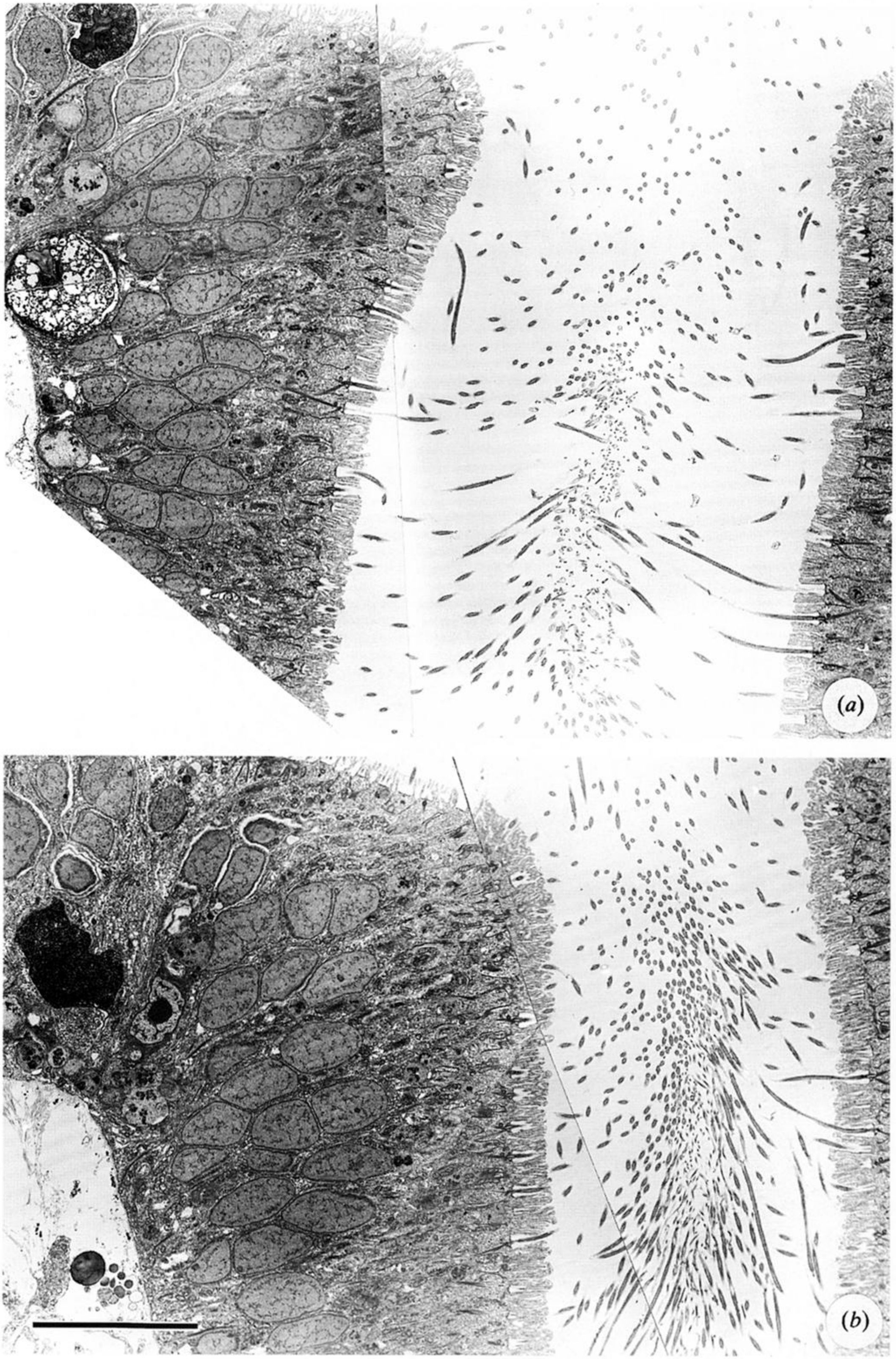

Figure 8. Transmission electron micrographs of vertical sections of: (*a*) a pore canal fixed without a CCh treatment; and (*b*) a pore canal fixed after a CCh treatment. Bar represents 10 μm.

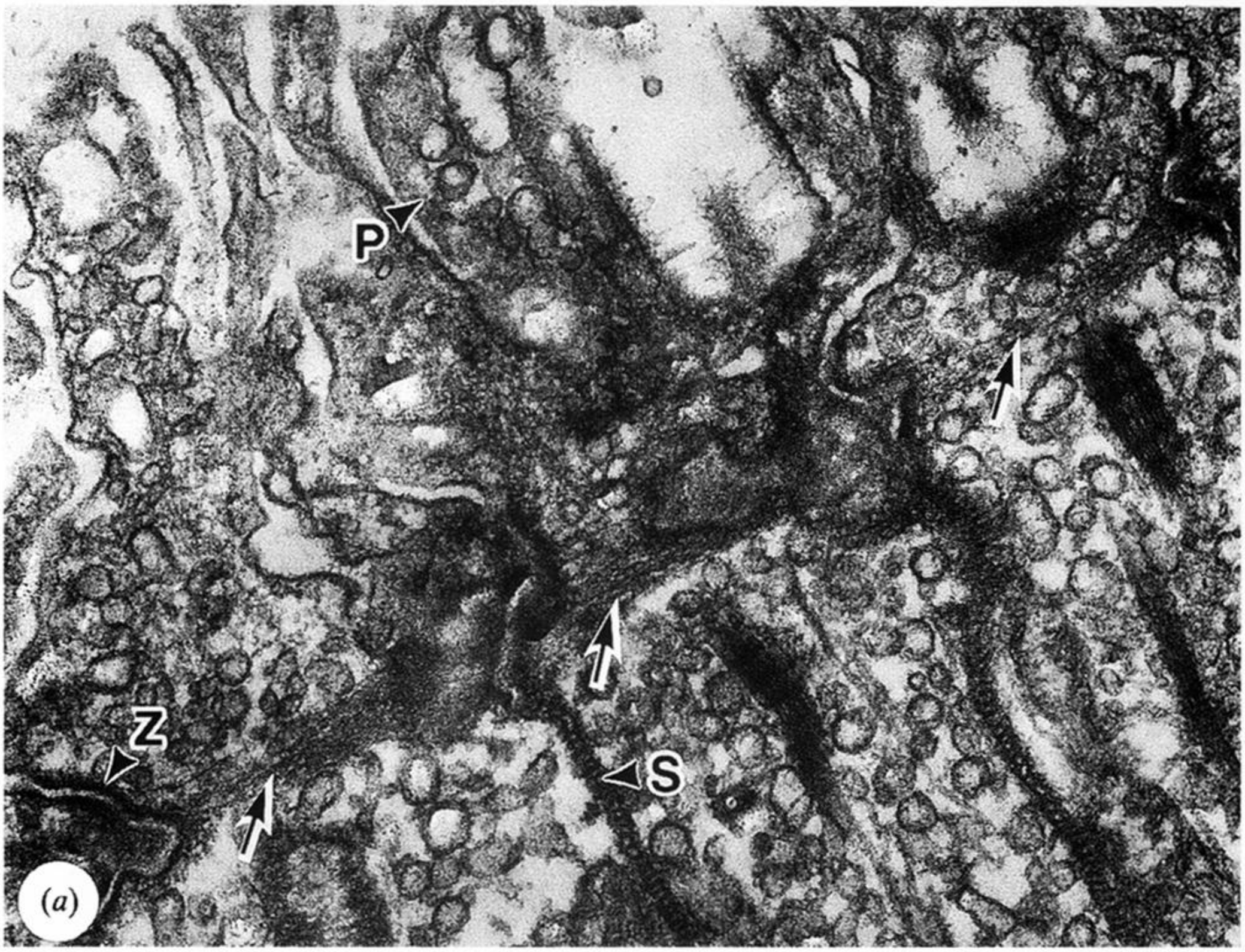

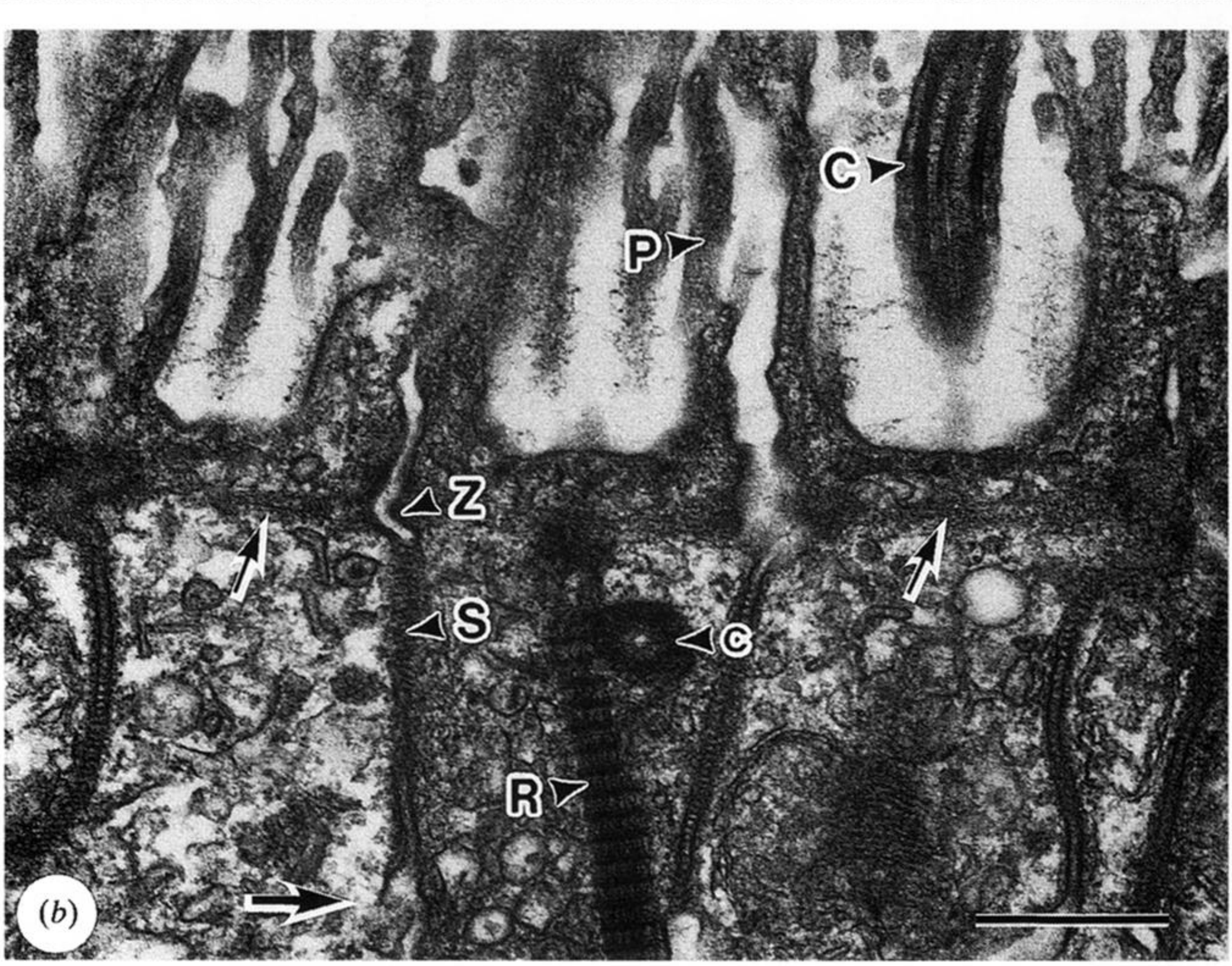

Figure 9. Transmission electron micrographs of apical regions of cells lining the lumen of the pore canal. (*a*) Horizontal section. (*b*) Vertical section. The smaller arrows indicate the filaments linking the adherens junctions. The larger arrow in (*b*) indicates the direction of the outer (aboral) surface. P: collar-like projection of the cell. S: septate junction. Z: adherens junction (*zonula adherens*). C: cilium. R: ciliary rootlet. c: centriole. Bar represents 0.5 μm.

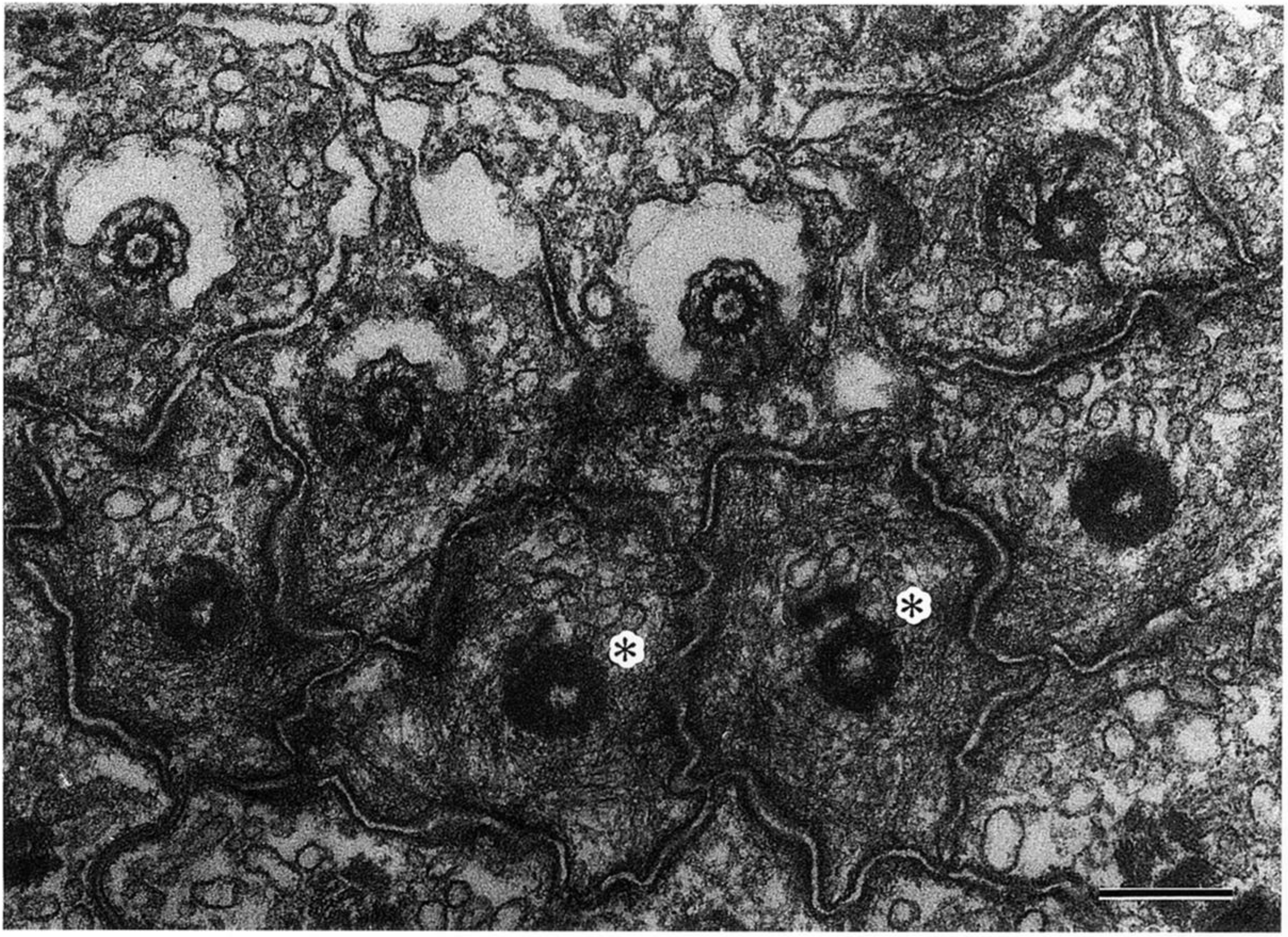

Figure 10. Transverse section of the pore-canal cells near their apical surface. Note the filaments circularly running just beneath the adherens junctions (e.g. in the cells marked with *). Bar represents 0.5 μm.

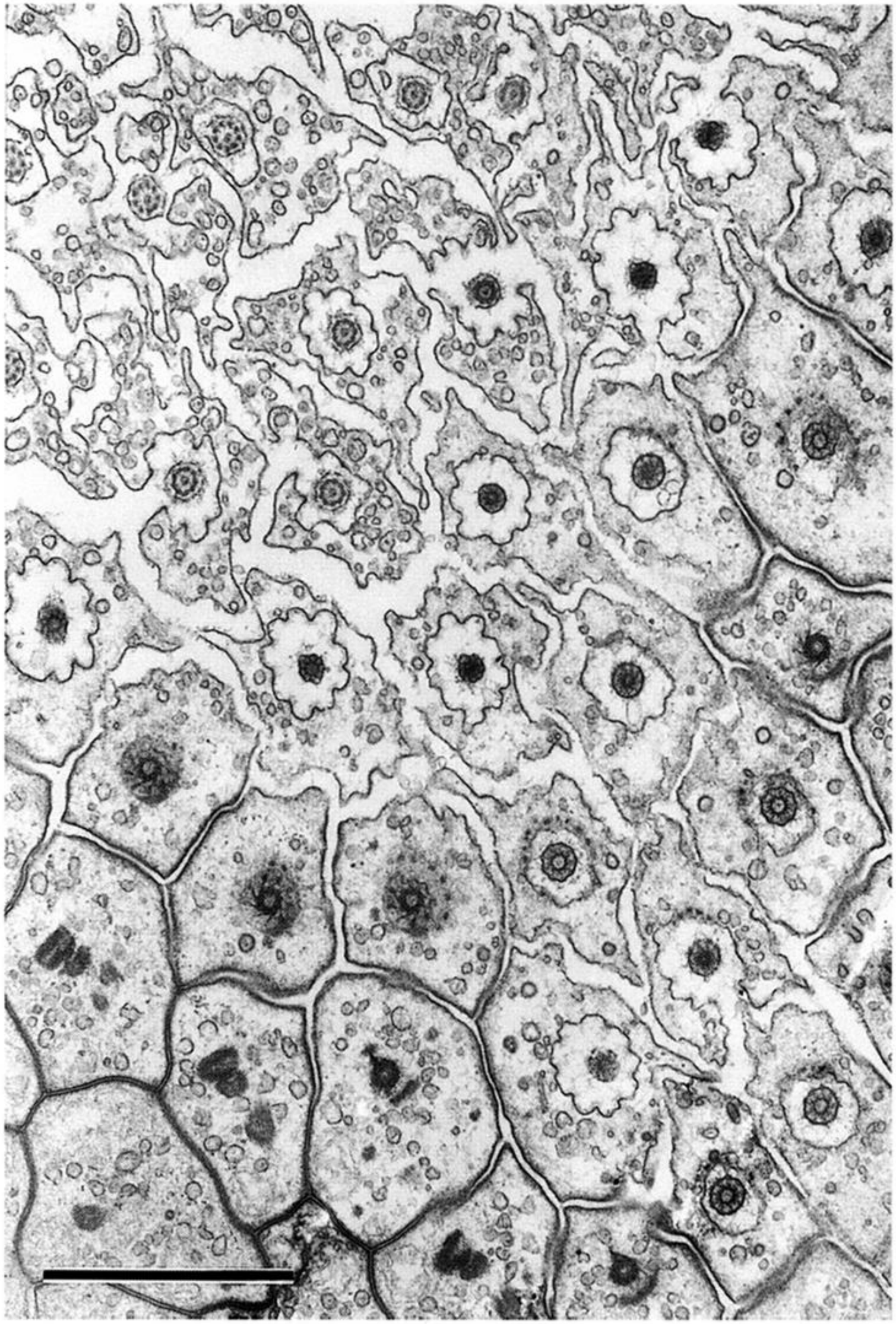

Figure 11. Tangential section of the luminal wall. A collar-like projection of the pore-canal cell surrounds the base of each cilium. Bar represents 2 μm.

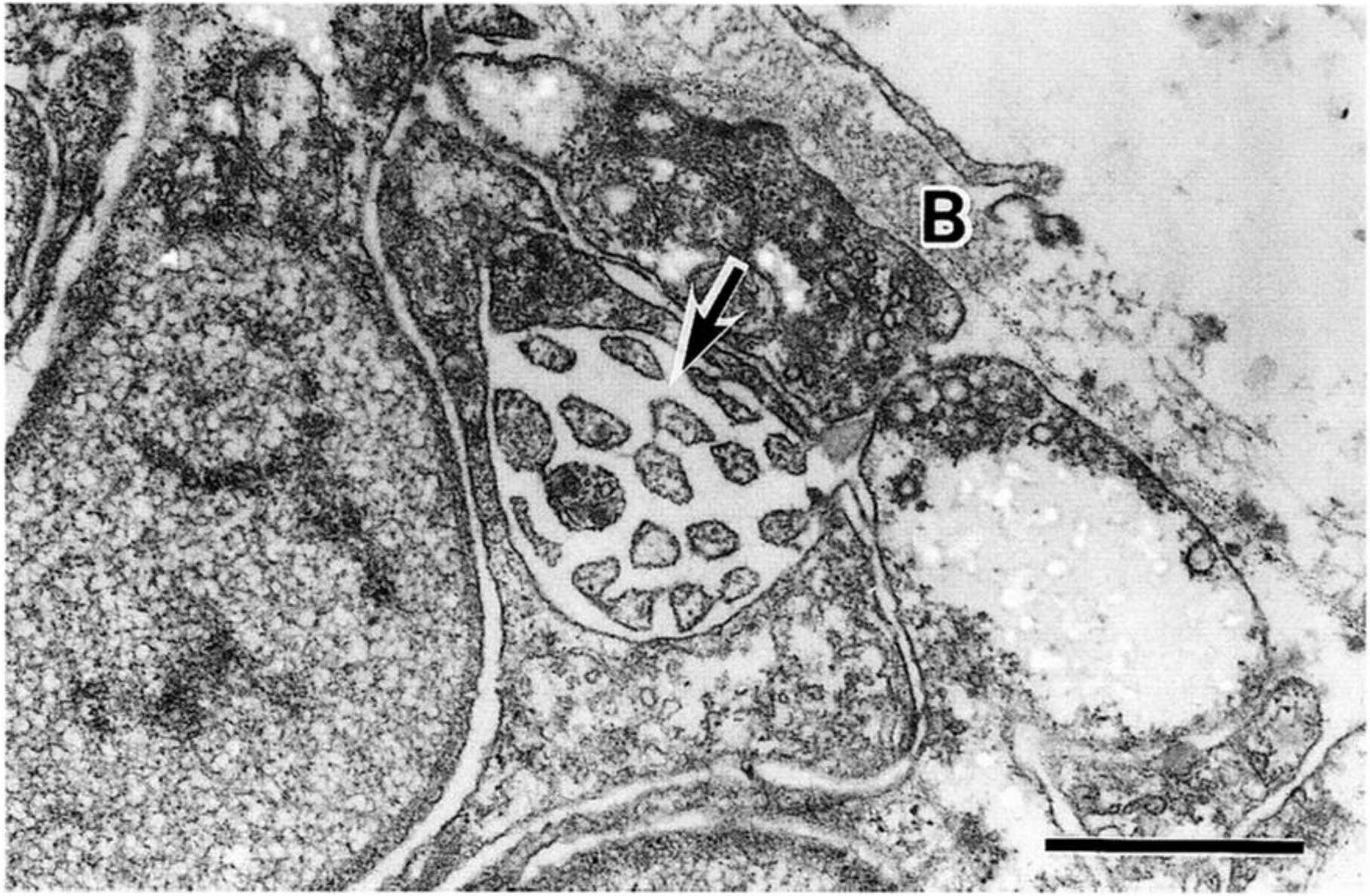

Figure 12. Horizontal section near the base of the pore canal showing the clusters of cell processes (arrow) between the pore-canal cell and the basal lamina (B). These processes are possibly a bundle of nerve fibres. Bar represents 1 μm.

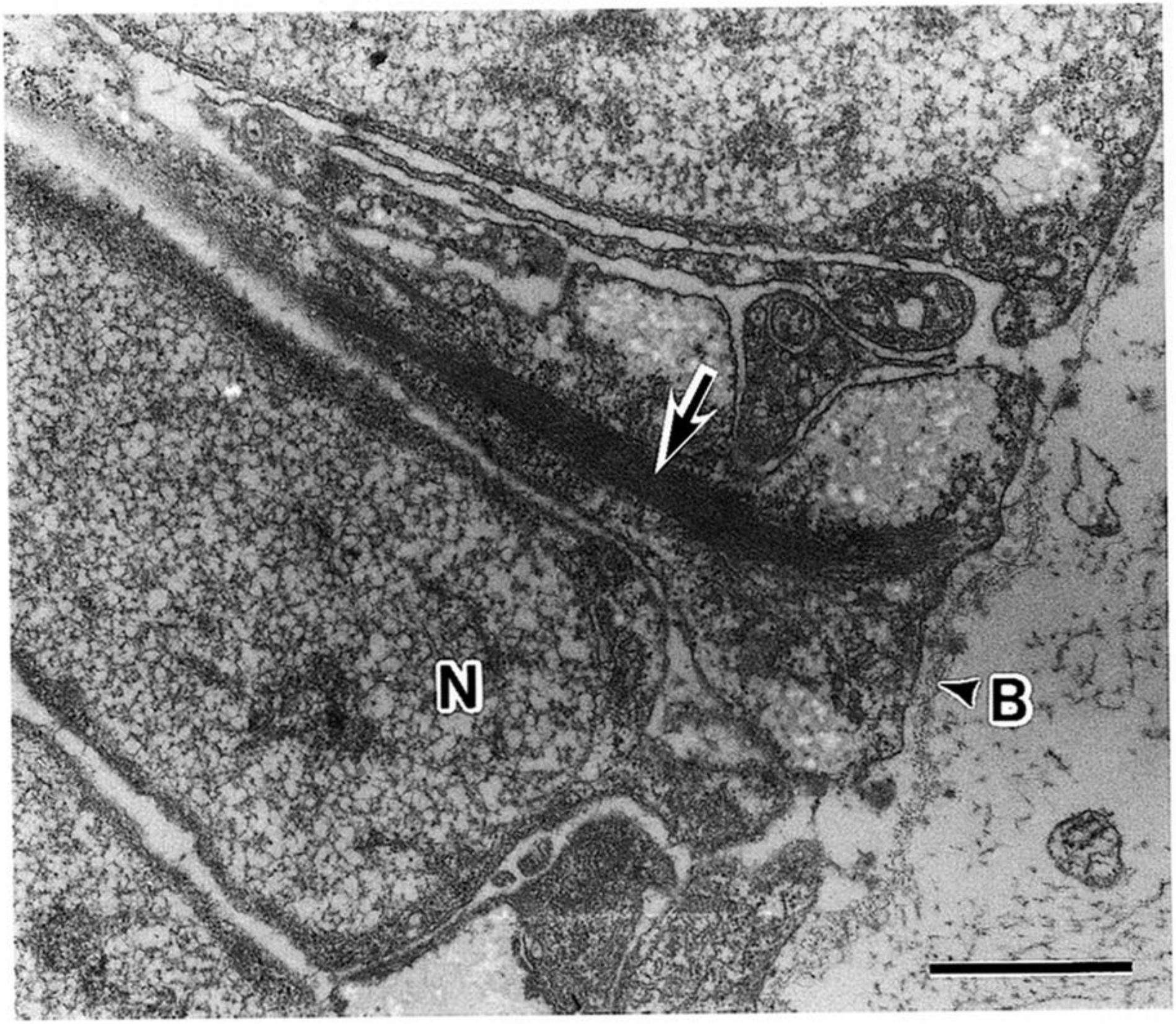

Figure 13. Vertical section at the base of the pore canal showing a bundle of filaments (arrow). B: basal lamina. N: nucleus. Bar represents 1 μm.

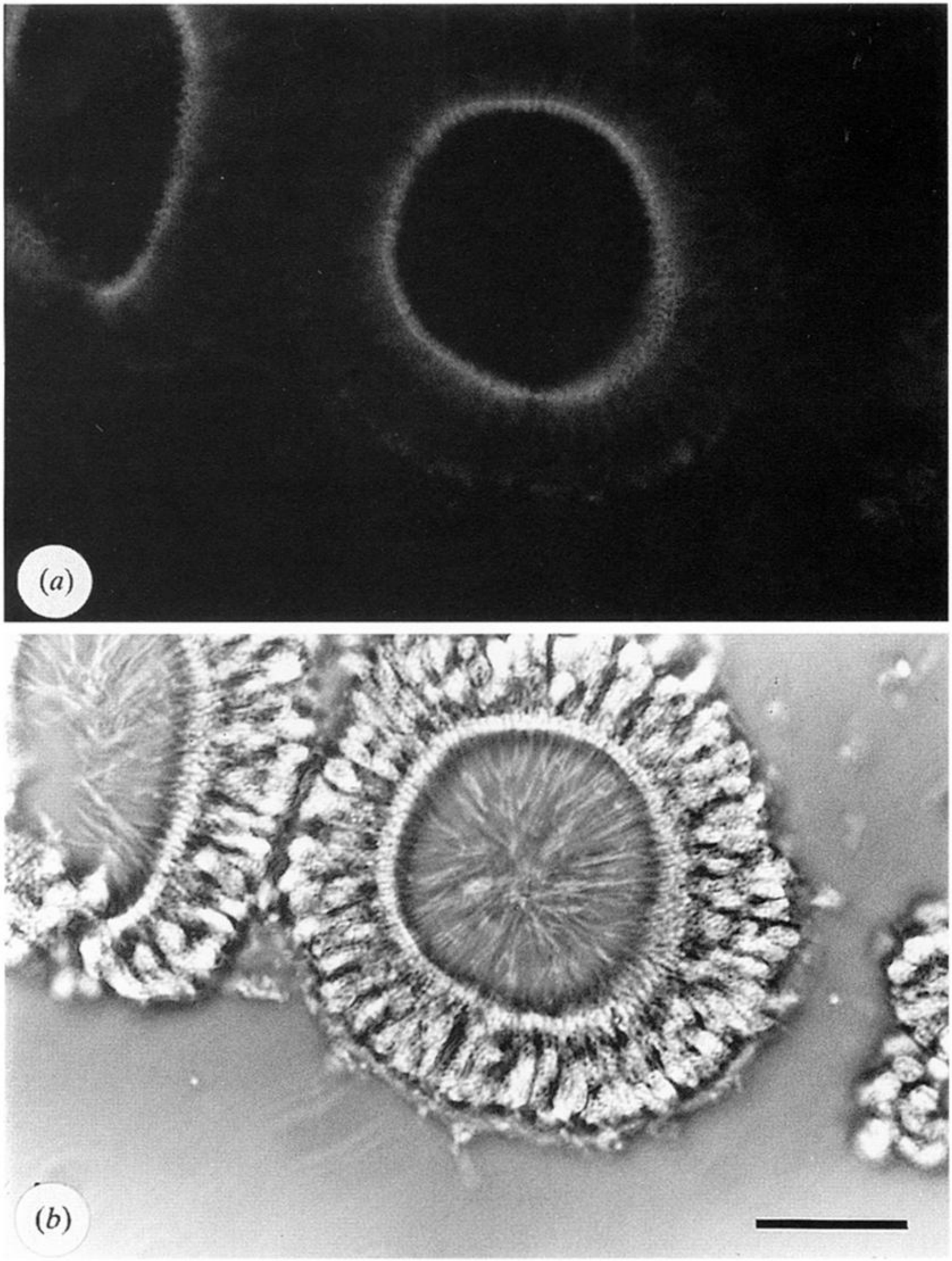

Figure 15. A cross section of pore canals stained with rhodamine-phalloidin. (*a*) Fluorescent light micrograph. (*b*) Phase contrast micrograph. Bar represents 20 μm.

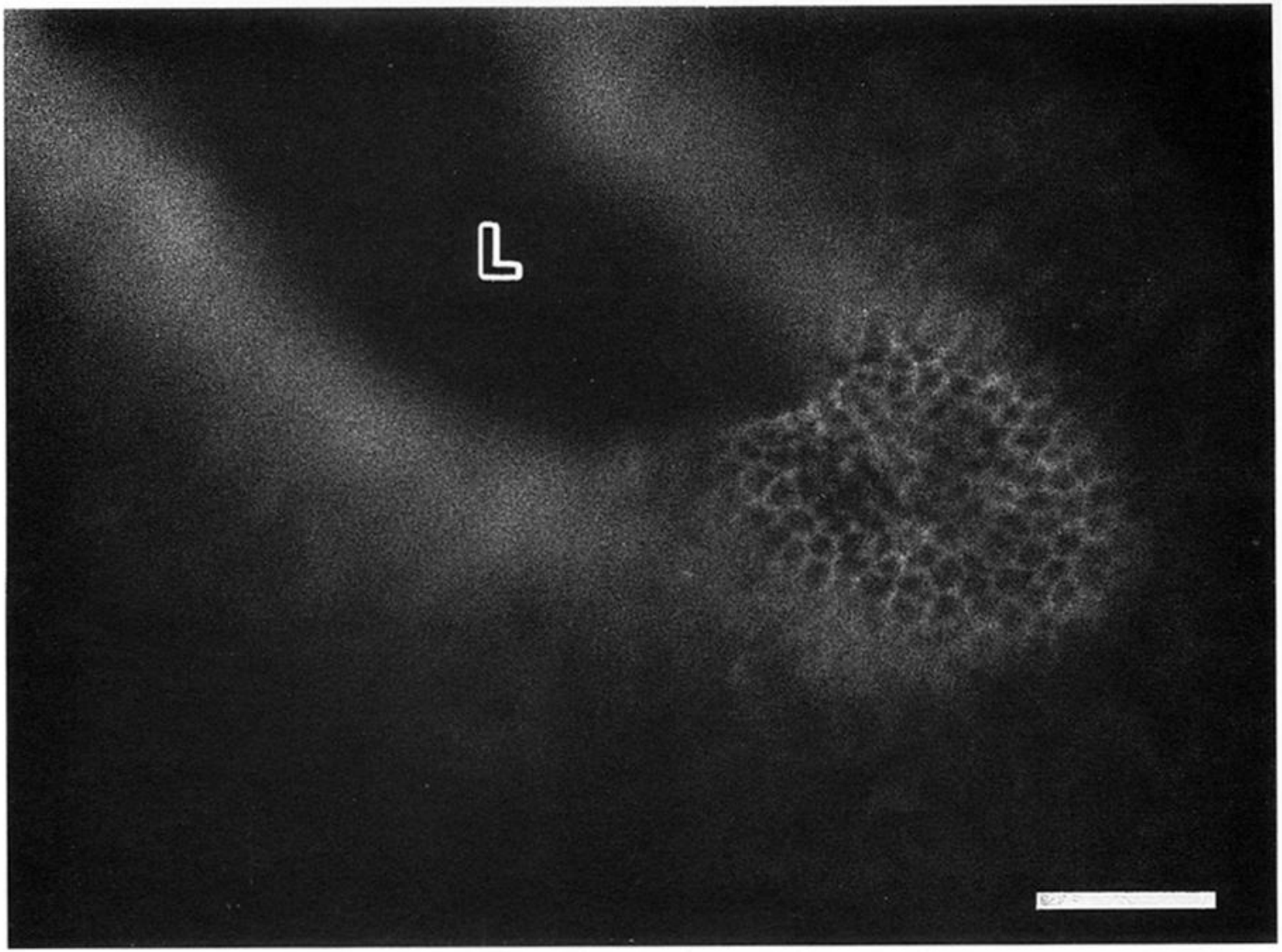

Figure 16. A fluorescent micrograph of a grazing section of a pore canal stained with rhodamine-phalloidin. The region near the luminal surface of the canal is found to be encircled by the fluorescent label and divided into many blocks. Each block seems to correspond to the apical part of each cell. The labelled region seems to correspond to the one where filaments are found by TEM. L: lumen of the pore canal. Bar represents 10 μm.